

A POSTERIORI ERROR ESTIMATORS FOR FOURTH ORDER ELLIPTIC PROBLEMS WITH CONCENTRATED LOADS

HUIHUI CAO[†], YUNQING HUANG[†], NIANYU YI[†], PEIMENG YIN^{†,*}

ABSTRACT. In this paper, we study two residual-based a posteriori error estimators for the C^0 interior penalty method in solving the biharmonic equation in a polygonal domain under a concentrated load. The first estimator is derived directly from the model equation without any post-processing technique. We rigorously prove the efficiency and reliability of the estimator by constructing bubble functions. Additionally, we extend this type of estimator to general fourth-order elliptic equations with various boundary conditions. The second estimator is based on projecting the Dirac delta function onto the discrete finite element space, allowing the application of a standard estimator. Notably, we additionally incorporate the projection error into the standard estimator. The efficiency and reliability of the estimator are also verified through rigorous analysis. We validate the performance of these a posteriori estimates within an adaptive algorithm and demonstrate their robustness and expected accuracy through extensive numerical examples.

1. INTRODUCTION

In this paper, we are interested in an adaptive C^0 interior penalty method for the biharmonic problem in polygonal domain $\Omega \subset \mathbb{R}^2$ with a concentrated load [36, 12]

$$\Delta^2 u = \delta_{\mathbf{x}_0} \quad \text{in } \Omega, \quad u = 0 \quad \text{and} \quad \partial_{\mathbf{n}} u = 0 \quad \text{on } \partial\Omega. \quad (1.1)$$

The boundary conditions are known as homogeneous Dirichlet boundary conditions or clamped boundary conditions [26], where $\partial_{\mathbf{n}} u$ denotes the outward normal derivative of u on $\partial\Omega$. $\delta_{\mathbf{x}_0}$ is a Dirac delta function concentrated at a point $\mathbf{x}_0 \in \Omega_0 \subset \Omega$ satisfying

$$\langle \delta_{\mathbf{x}_0}, v \rangle = v(\mathbf{x}_0), \quad \forall v \in C(\Omega_0).$$

Elliptic problems with Dirac delta source terms are encountered in various applications, such as the electric field generated by a point charge, transport equations for effluent discharge in aquatic media, modeling of acoustic monopoles [24, 2, 28, 19]. The biharmonic problem can be used to study the small deflections of a thin plate, especially the biharmonic problem (1.1) with the Dirac delta source term describes the deflections for thin plates with a concentrated load [36, 12].

The Dirac measure in (1.1) does not belong to $H^{-1}(\Omega)$, resulting in the solution exhibiting low regularity. Analytical solutions for biharmonic problem (1.1) are typically challenging, though they exist for some special cases of geometry and loads. For example, analytical methods for the biharmonic problem (1.1) have primarily focused on circular and annular domains (see, e.g., [36, 12, 15]). Consequently, numerical methods have garnered widespread attention for solving (1.1), such as the boundary element method [12], the regular hybrid boundary node method [37]. Discussion on various numerical methods for biharmonic problem (1.1) can be found in [37] and the references therein. Among various numerical methods, the finite element method is the most popular.

Key words and phrases. Dirac delta function; C^0 interior penalty method; a posteriori error estimators; adaptive algorithm; efficiency and reliability.

* Corresponding author.

Finite element methods developed for the general biharmonic equation with Dirichlet boundary conditions can typically be applied to solve the specific biharmonic problem (1.1). The conforming finite element method is one approach, where the presence of high-order derivatives necessitates finite element spaces that belong to H^2 , such as the C^1 Argyris finite element method [3]. Additionally, the general biharmonic problem can be decomposed into Poisson and Stokes equations, which are then solved using the C^0 finite element method [29]. However, whether this decomposition strategy is effective for problem (1.1) remains to be explored since such decomposition requires the source term in $H^{-1}(\Omega)$ or its subset. Another option that utilizes the C^0 finite element space, yet can still accommodate singular source terms not in $H^{-1}(\Omega)$, is the C^0 interior penalty method [17]. Its stability is ensured by penalty terms enforced across the mesh cell interfaces.

For the biharmonic problem (1.1), some finite element methods and error analyses are available in the literature. A C^1 finite element approximation was proposed in [33], and optimal error estimates were studied on quasi-uniform meshes, in which the H^2 error estimate is of order h when using polynomials of degree greater than 2. More recently, a C^0 interior penalty method was studied in [27], and a local H^2 error estimate of order $|\ln h|^{\frac{3}{2}}$ was given on quasi-uniform meshes. Due to the low regularity of the solution, the convergence rates on quasi-uniform meshes are inherently limited. To improve the convergence rate in the finite element approximation, adopting an adaptive finite element method becomes necessary. Thus, the primary objective of this paper is to develop an adaptive C^0 interior penalty method for the biharmonic problem (1.1).

Many adaptive finite element methods are available for second order elliptic equations with Dirac delta source term. Though $\delta_{\mathbf{x}_0}$ is not in $H^{-1}(\Omega)$ and $u \notin H^1(\Omega)$, the C^0 finite element method can still approximate the equations. However, direct application of the residual-based a posteriori error estimator using standard energy norms is not viable. In the literature, two typical strategies have been studied to address this issue. One approach is to utilize norms weaker than $H^1(\Omega)$ for error estimation. For instance, Araya et al. [1] derived a posteriori error estimators in $L^p(1 < p < \infty)$ norm and $W^{1,p}(p_0 < p < 2, p_0 \in [1, 2))$ seminorms for a Poisson problem with a Dirac delta source term on two-dimensional domains. Gaspoz et al. [21] provided a posteriori error estimates in $H^{1-s}, s \in (0, \frac{1}{2})$ norm. Additionally, a global upper bound and a local lower bound of residual type a posteriori error estimators in a weighted Sobolev norm $\|\cdot\|_{H_\alpha^1}$ with $\alpha \in (\frac{d}{2} - 1, \frac{d}{2})$ (d is the spatial dimension) for elliptic problems were obtained by Agmon et al. in [4]. Another is to regularize the source term to an $L^2(\Omega)$ function by projecting it onto a polynomial space, potentially introducing a projection error. This regularization allows the application of standard residual-based a posteriori error estimators for general Poisson problems. For further insights, readers are referred to early review articles, such as [23, 31].

Results on a posteriori error estimates of the C^0 interior penalty method for biharmonic problems with $L^2(\Omega)$ source terms can be found in [22]. However, no result is available for the fourth order elliptic equation with the Dirac delta source term, which does not belong to $H^{-1}(\Omega)$, not to mention in $L^2(\Omega)$. Therefore, to improve the accuracy of the numerical solution while optimizing the distribution of computational resources, we propose two types of residual-based a posteriori error estimators for the biharmonic problem (1.1) to guide mesh adaptive refinement around singular points.

The first type of a posterior error estimator is derived based on the primal equation (1.1). Depending on the location of \mathbf{x}_0 in the computational element, this error estimator can take different forms. Specifically, if \mathbf{x}_0 is not a vertex, an additional term that depends on the size of the element will be required. We rigorously prove the upper and lower bounds of the proposed estimator to ensure its reliability and

efficiency. Moreover, we extend this residual-type a posteriori error estimator to fourth-order elliptic equations with various boundary conditions.

The second type of a posteriori error estimator is proposed based on the projection techniques. We first project $\delta_{\mathbf{x}_0}$ onto δ_h in the finite element space, and then use this projection δ_h to construct a residual-type a posteriori error estimator. This method introduces an additional error between δ_h and $\delta_{\mathbf{x}_0}$, which is shown to be of the same order as the finite element approximation. Therefore, it does not compromise the accuracy of the numerical solution. This is further supported by our error analysis and numerical experimental results.

The rest of the paper is organized as follows. In Section 2, we establish the well-posedness and discrete problem of (1.1) by the C^0 interior penalty method. The main results are presented in Section 3, where we propose two types of residual-based a posteriori error estimators, upper and lower bounds are proved in order to guarantee the reliability and the efficiency of the proposed estimators. In Section 4, we extend our results to a broader class of fourth-order elliptic equations with various boundary conditions. Section 5 provides numerous numerical examples to illustrate the robustness of our estimators and the corresponding adaptive C^0 interior penalty method. Finally, we draw some conclusions in Section 6.

Throughout the paper, the generic constant $C > 0$ in our estimates may differ at different occurrences. It will depend on the computational domain, but not on the functions involved or on the mesh level in the finite element algorithms.

2. PRELIMINARIES AND C^0 INTERIOR PENALTY METHOD

Denote by $H^m(\Omega)$, m is a non-negative integer, the Sobolev space that consists of functions whose i th ($0 \leq i \leq m$) derivatives are square integrable. Let $L^2(\Omega) := H^0(\Omega)$. Denote by $H_0^1(\Omega) \subset H^1(\Omega)$ the subspace consisting of functions with zero trace on the boundary $\partial\Omega$. For $0 < t < 1$ and $s = m + t$, the fractional order Sobolev space $H^s(D)$ consists of distributions $v \in D \subset \mathbb{R}^d$ ($d = 1, 2$) satisfying

$$\|v\|_{H^s(D)}^2 := \|v\|_{H^m(D)}^2 + \sum_{|\nu|=m} \int_D \int_D \frac{|\partial^\nu v(x) - \partial^\nu v(y)|^2}{|x - y|^{d+2t}} dx dy < \infty,$$

where $\nu = (\nu_1, \dots, \nu_d) \in \mathbb{Z}_{\geq 0}^d$ is a multi-index such that $\partial^\nu = \partial_{x_1}^{\nu_1} \cdots \partial_{x_d}^{\nu_d}$ and $|\nu| = \sum_{i=1}^d \nu_i$.

2.1. Well-posedness and regularity. We first show the well-posedness of the problem (1.1).

Lemma 2.1. For any $\epsilon > 0$, it follows that the point Dirac delta function $\delta_{\mathbf{x}_0} \in H^{-1-\epsilon}(\Omega)$ and satisfies

$$\|\delta_{\mathbf{x}_0}\|_{H^{-1-\epsilon}(\Omega)} \leq C.$$

Proof. For any $v \in H^{1+\epsilon}(\Omega)$, the embedding theorem [13] implies that $v \in C^{0,\epsilon}(\Omega) \subset C^0(\Omega)$. Then,

$$|\langle \delta_{\mathbf{x}_0}, v \rangle| = |v(\mathbf{x}_0)| \leq \|v\|_{L^\infty(\Omega)} \leq C \|v\|_{H^{1+\epsilon}(\Omega)},$$

and

$$\|\delta_{\mathbf{x}_0}\|_{H^{-1-\epsilon}(\Omega)} := \sup_{v \in H^{1+\epsilon}(\Omega) \setminus \{0\}} \frac{|\langle \delta_{\mathbf{x}_0}, v \rangle|}{\|v\|_{H^{1+\epsilon}(\Omega)}} \leq C.$$

□

The variational formulation for problem (1.1) is to find $u \in H_0^2(\Omega)$, such that

$$a(u, v) := \int_{\Omega} \Delta u \Delta v \, d\mathbf{x} = \langle \delta_{\mathbf{x}_0}, v \rangle, \quad \forall v \in H_0^2(\Omega). \quad (2.1)$$

The Sobolev imbedding theorem [30] implies $v \in C(\Omega)$ for $v \in H_0^2(\Omega)$, thus the variational formulation (2.1) is well-posed.

We sketch a drawing of the domain Ω with a singular point \mathbf{x}_0 in Figure 1. We assume the largest interior angle $\omega \in [\frac{\pi}{3}, 2\pi)$ of the domain associated with the vertex Q . For simplicity of the analysis, we assume that

$$\sin \sqrt{\frac{\omega^2}{\sin^2 \omega} - 1} \neq \sqrt{1 - \frac{\sin^2 \omega}{\omega^2}}. \quad (2.2)$$

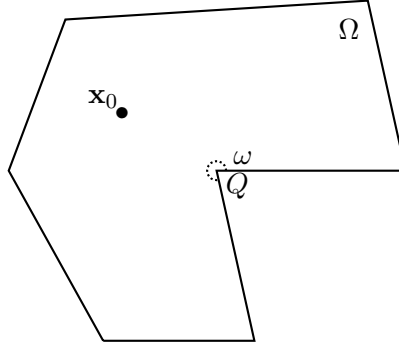


FIGURE 1. Domain Ω with interior angle ω contains a singular point \mathbf{x}_0 .

Let z_ℓ , $\ell = 1, 2, \dots$ satisfying $\text{Re}(z_\ell) > 0$ be the solutions of the following characteristic equation

$$\sin^2(z\omega) = z^2 \sin^2(\omega). \quad (2.3)$$

Then there exists a threshold

$$\alpha_0 := \min\{\text{Re}(z_\ell), \ell = 1, 2, \dots, \} > \frac{1}{2}, \quad (2.4)$$

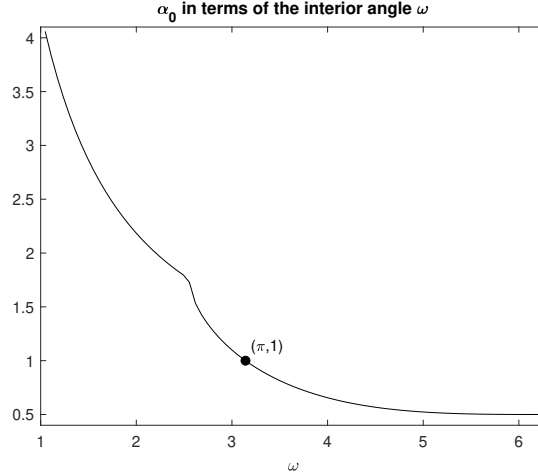
such that the following regularity result holds.

Lemma 2.2. For any $\epsilon > 0$, let u be the solution of the biharmonic problem (1.1). Then it follows $u \in H^{\min\{3-\epsilon, 2+\alpha\}}(\Omega) \cap H_0^2(\Omega)$ with $\frac{1}{2} < \alpha < \alpha_0$. Moreover, if $\omega < \pi$, it holds $u \in H^{3-\epsilon}(\Omega) \cap H_0^2(\Omega)$; and if $\omega > \pi$, it holds $u \in H^{2+\alpha}(\Omega) \cap H_0^2(\Omega)$.

The graph of α_0 in terms of the largest interior angle ω is shown in Figure 2, and some numerical values of α_0 are shown in Table 1 [29]. In Lemma 2.2, when $\omega < \pi$, the regularity is dominated by the singularity of the Dirac delta source; and when $\omega > \pi$, the regularity is dominated by the singularity of the domain [25, 5, 6, 18]. To design high-order accurate numerical methods, one has to handle the singularities introduced by these two singular sources: domain corner, and Dirac delta source.

TABLE 1. Values of α_0 for different interior angles ω .

ω	$\frac{\pi}{3}$	$\frac{\pi}{2}$	$\frac{2\pi}{3}$	$\frac{3\pi}{4}$	$\frac{5\pi}{6}$	$\frac{11\pi}{12}$	$\frac{7\pi}{6}$	$\frac{6\pi}{5}$	$\frac{5\pi}{4}$	$\frac{4\pi}{3}$	$\frac{3\pi}{2}$	$\frac{7\pi}{4}$
$\alpha_0 \approx$	4.0593	2.7396	2.0941	1.8854	1.5339	1.2006	0.7520	0.7178	0.6736	0.6157	0.5445	0.5050

FIGURE 2. α_0 in terms of the largest interior angle ω .

2.2. C^0 interior penalty method. Let \mathcal{T}_h be a triangulation of domain Ω satisfying $\bar{\Omega} = \sum_{K \in \mathcal{T}_h} \bar{K}$. We denote the sets of interior and boundary edges of \mathcal{T}_h by \mathcal{E}_I and \mathcal{E}_B , respectively. We also set $\mathcal{E}_h = \mathcal{E}_I \cup \mathcal{E}_B$. We further denote the mesh size of $K \in \mathcal{T}_h$ by $h_K = \text{diam}(K)$, and denote by $h = \max_{K \in \mathcal{T}_h} h_K$. The length of an edge $e \in \mathcal{E}_h$ is denoted by h_e . Here special attention has to be paid that the elements of \mathcal{T}_h are shape-regular, it implies that mesh \mathcal{T}_h is locally quasi-uniform, i.e., if two elements K_i and K_j satisfy $\bar{K}_i \cap \bar{K}_j \neq \emptyset$, there exists a constant $C > 1$ such that,

$$C^{-1}h_{K_i} \leq h_{K_j} \leq Ch_{K_i}. \quad (2.5)$$

Throughout the paper, we denote $K_0 \in \mathcal{T}_h$ by one element such that the singular point $\mathbf{x}_0 \in \bar{K}_0$, where \bar{K}_0 is the closure of K_0 . If \mathbf{x}_0 lies on an inner edge, either of the two triangles sharing that edge can be chosen as K_0 . Similarly, if \mathbf{x}_0 is a vertex of several triangles, any one of these triangles can be chosen as K_0 . The diameter of K_0 is denoted by h_{K_0} .

We define the broken Sobolev space $H^r(\Omega, \mathcal{T}_h)$ associated with the triangulation \mathcal{T}_h by

$$H^r(\Omega, \mathcal{T}_h) = \{v \in L^2(\Omega) : v|_K \in H^r(K), \quad \forall K \in \mathcal{T}_h\}.$$

The space $H^r(\Omega, \mathcal{T}_h)$ equipped with the broken Sobolev norm and seminorm

$$\|u\|_{r, \mathcal{T}_h} = \left(\sum_{K \in \mathcal{T}_h} \|u\|_{H^r(K)}^2 \right)^{\frac{1}{2}}, \quad |u|_{r, \mathcal{T}_h} = \left(\sum_{K \in \mathcal{T}_h} |u|_{H^r(K)}^2 \right)^{\frac{1}{2}}$$

The C^0 finite element space is

$$V_{h,0}^m = \{v_h \in H_0^1(\Omega) \cap C^0(\Omega) : v_h|_K \in P_m(K), \quad m \geq 2, \quad \forall K \in \mathcal{T}_h\}, \quad (2.6)$$

where $P_m(K)$ is the space of polynomials of degree less than or equal to m on element K .

For each $e \in \mathcal{E}_I$, we denote K^+ and K^- by two adjacent triangles that share one common edge e . The unit outward normal vector \mathbf{n} is oriented from K^+ to K^- . We may designate as K^+ that with the higher of the indices. When $e \in \mathcal{E}_B$, let K^+ be the element with the edge e and denote by \mathbf{n} a unit outward normal vector to ∂K^+ . For any $e \in \mathcal{E}_h$, denote by v^+ and v^- the two traces of v along the edge e . For

a scalar function v and a vector function \mathbf{q} that may be discontinuous across e , we define the following jumps:

$$\llbracket \mathbf{q} \rrbracket = \begin{cases} (\mathbf{q}^+ - \mathbf{q}^-) \cdot \mathbf{n}, & e \in \mathcal{E}_I, \\ \mathbf{q}^+ \cdot \mathbf{n}, & e \in \mathcal{E}_B, \end{cases} \quad \llbracket v \rrbracket = \begin{cases} (v^+ - v^-) \mathbf{n}, & e \in \mathcal{E}_I, \\ v^+ \mathbf{n}, & e \in \mathcal{E}_B, \end{cases}$$

and averages

$$\{\{\mathbf{q}\}\} = \begin{cases} \frac{1}{2}(\mathbf{q}^+ + \mathbf{q}^-), & e \in \mathcal{E}_I, \\ \mathbf{q}^+, & e \in \mathcal{E}_B. \end{cases} \quad \{\{v\}\} = \begin{cases} \frac{1}{2}(v^+ + v^-), & e \in \mathcal{E}_I, \\ v^+, & e \in \mathcal{E}_B. \end{cases}$$

According to above definition, for $\forall v \in H^r(\Omega, \mathcal{T}_h)$ and $\forall \mathbf{q} \in [H^r(\Omega, \mathcal{T}_h)]^2$, it is clearly that

$$\llbracket \mathbf{q} v \rrbracket = \{\{v\}\} \llbracket \mathbf{q} \rrbracket + \{\{\mathbf{q}\}\} \cdot \llbracket v \rrbracket. \quad (2.7)$$

The following identity can be verified by simple algebraic manipulation

$$\sum_{K \in \mathcal{T}_h} \int_{\partial K} v \mathbf{q} \cdot \mathbf{n} \, ds = \sum_{e \in \mathcal{E}_I} \int_e \{\{\mathbf{q}\}\} \cdot \llbracket v \rrbracket \, ds + \sum_{e \in \mathcal{E}_h} \int_e \{\{v\}\} \llbracket \mathbf{q} \rrbracket \, ds. \quad (2.8)$$

The C^0 interior penalty method for (1.1) is to find $u_h \in V_{h,0}^m$ such that [32]

$$A_h(u_h, v_h) = v_h(\mathbf{x}_0) \quad \forall v_h \in V_{h,0}^m, \quad (2.9)$$

where the bilinear form

$$\begin{aligned} A_h(u_h, v_h) := & \sum_{K \in \mathcal{T}_h} \int_K \Delta u_h \Delta v_h \, dx - \sum_{e \in \mathcal{E}_h} \left(\int_e \{\{\Delta u_h\}\} \llbracket \nabla v_h \rrbracket \, ds + \int_e \{\{\Delta v_h\}\} \llbracket \nabla u_h \rrbracket \, ds \right) \\ & + \sum_{e \in \mathcal{E}_h} \frac{\beta}{h_e} \int_e \llbracket \nabla u_h \rrbracket \llbracket \nabla v_h \rrbracket \, ds. \end{aligned} \quad (2.10)$$

Here, the penalty parameter β needs to be large enough to ensure the stability of the C^0 interior penalty method. Define the energy norm by

$$\| \| v \| \|^2 := a_h(v, v) + \sum_{e \in \mathcal{E}_h} \frac{\beta}{h_e} \| \llbracket \nabla v \rrbracket \|_{L^2(e)}^2, \quad \forall v \in H^2(\Omega, \mathcal{T}_h), \quad (2.11)$$

where

$$a_h(u, v) := \sum_{K \in \mathcal{T}_h} \int_K \Delta u \Delta v \, dx.$$

It can be observed that $\| \| \cdot \| \|$ defines a norm on the space $H^2(\Omega, \mathcal{T}_h)$.

Recall that $a(\cdot, \cdot)$ is defined in (2.1), we can observe that

$$a_h(v, v) = a(v, v) \approx |v|_{H^2(\Omega)}^2, \quad \forall v \in H_0^2(\Omega). \quad (2.12)$$

The statement \approx represents equivalence. Then the following inequalities hold.

Lemma 2.3 (Continuity and coercivity [32]). For sufficiently large β , there exists positive constants C_s and C_b for the bilinear form (2.10), such that

$$|A_h(u_h, v_h)| \leq C_b \| \| u_h \| \| * \| \| v_h \| \|, \quad \forall u_h, v_h \in V_{h,0}^m, \quad (2.13)$$

$$A_h(v_h, v_h) \geq C_s \| \| v_h \| \|^2, \quad \forall v_h \in V_{h,0}^m. \quad (2.14)$$

By Lemma 2.3 and the Lax–Milgram Theorem, the discretized problem (2.9) admits a unique solution.

2.3. A priori error estimate. Given the regularity outlined in Lemma 2.2, we review the following results, which are extensively used in the a priori and a posteriori error estimates.

Lemma 2.4 (Trace inequality [11]). For any element $K \in \mathcal{T}_h$ and $e \subset \partial K$, it follows

$$\begin{aligned} \|v\|_{L^2(e)} &\leq Ch_K^{-1/2} (\|v\|_{L^2(K)} + h_K \|\nabla v\|_{L^2(K)}), & \forall v \in H^1(K), \\ \|\partial_{\mathbf{n}} v\|_{L^2(e)} &\leq Ch_K^{-1/2} (\|\nabla v\|_{L^2(K)} + h_K \|\nabla^2 v\|_{L^2(K)}), & \forall v \in H^2(K). \end{aligned}$$

Lemma 2.5 (Inverse inequality [11]). For any element $K \in \mathcal{T}_h$, $v \in P_m(K)$, and $e \subset \partial K$, it follows

$$\begin{aligned} \|v\|_{L^2(e)} &\leq Ch_K^{-1/2} \|v\|_{L^2(K)}, \\ \|\partial_{\mathbf{n}} v\|_{L^2(e)} &\leq Ch_K^{-1/2} \|\nabla v\|_{L^2(K)}, \\ \|\nabla^j v\|_{L^2(K)} &\leq Ch_K^{-j} \|v\|_{L^2(K)}, \quad \forall 0 \leq j \leq m. \end{aligned}$$

Lemma 2.6 (Interpolation error estimate [7]). Let $\Pi_h : H_0^2(\Omega) \rightarrow V_{h,0}^m$ be the standard Lagrange nodal interpolation operator, then it follows

$$\begin{aligned} |\phi - \Pi_h \phi|_{H^l(K)} &\leq Ch_K^{2-l} |\phi|_{H^2(K)}, \quad 0 \leq l \leq 2, \\ |\phi - \Pi_h \phi|_{H^r(\partial K)} &\leq Ch_K^{3/2-r} |\phi|_{H^2(K)}, \quad r = 0, 1. \end{aligned}$$

Based on the preparations above and the analysis in [8], the following a priori error estimate can be derived for the solution of the C^0 interior penalty method.

Lemma 2.7. Let $u \in H_0^2(\Omega)$ be the solution of equation (1.1), and u_h be the approximation solution of (2.9). Then it follows

$$\|u - u_h\| \leq Ch^{\min\{1-\epsilon, \alpha\}} \|u\|_{H^{\min\{3-\epsilon, 2+\alpha\}}(\Omega)}, \quad (2.15)$$

where $\alpha < \alpha_0$ with α_0 given in (2.4).

3. RESIDUAL-BASED A POSTERIORI ERROR ESTIMATORS

To improve the convergence rate of the C^0 interior penalty method in Lemma 2.7, we propose an adaptive C^0 interior penalty method in this section. Specifically, we introduce two residual-type a posteriori error estimators for problem (1.1). Based on the derived error estimators and a bisection mesh refinement method, we then develop an adaptive C^0 interior penalty algorithm.

3.1. A posteriori error estimation based on primal problem. The first type of error estimator is obtained in a straightforward manner based on the problem (1.1). Theoretically, we establish upper and lower bounds to ensure the reliability and efficiency of the proposed estimator.

Let $u_h \in V_{h,0}^m$ be the approximation solution obtained by the C^0 interior penalty method (2.9) for problem (1.1). For each $K \in \mathcal{T}_h$, \mathcal{E}_K represents the set of three edges of element K . Denote the set of all mesh nodes of the triangulation \mathcal{T}_h by \mathcal{N} . The number of nodes is equal to the degrees of freedom. For example, \mathcal{N} includes vertices and edge center points for the quadratic polynomial approximation. We propose the following residual-based a posteriori error estimator on $K \in \mathcal{T}_h$ involving the location of the Dirac point in the mesh

$$\eta_K(u_h) = \begin{cases} (h_{K_0}^2 + \bar{\eta}_{K_0}^2)^{1/2}, & \text{if } K = K_0 \text{ and } \mathbf{x}_0 \notin \mathcal{N}, \\ \bar{\eta}_K, & \text{otherwise,} \end{cases} \quad (3.1)$$

where

$$\bar{\eta}_K(u_h) = \left(\eta_{1,K}^2 + \sum_{e \in \mathcal{E}_K \cap \mathcal{E}_h} \alpha_e \eta_{2,e}^2 + \sum_{e \in \mathcal{E}_K \cap \mathcal{E}_I} \alpha_e \eta_{3,e}^2 + \sum_{e \in \mathcal{E}_K \cap \mathcal{E}_I} \alpha_e \eta_{4,e}^2 \right)^{1/2}, \quad (3.2)$$

with $\alpha_e = 1$ for $e \in \mathcal{E}_B$, $\alpha_e = 1/2$ for $e \in \mathcal{E}_I$, and

$$\eta_{1,K} = h_K^2 \|\Delta^2 u_h\|_{L^2(K)}, \quad \eta_{2,e} = \beta h_e^{-1/2} \|[\nabla u_h]\|_{L^2(e)}, \quad (3.3)$$

$$\eta_{3,e} = h_e^{1/2} \|[\Delta u_h]\|_{L^2(e)}, \quad \eta_{4,e} = h_e^{3/2} \|[\nabla \Delta u_h]\|_{L^2(e)}. \quad (3.4)$$

Then the corresponding global error estimator is given by

$$\eta(u_h) = \begin{cases} \left(h_{K_0}^2 + \sum_{K \in \mathcal{T}_h} \eta_K^2(u_h) \right)^{1/2}, & \text{if } \mathbf{x}_0 \notin \mathcal{N}, \\ \left(\sum_{K \in \mathcal{T}_h} \eta_K^2(u_h) \right)^{1/2}, & \text{if } \mathbf{x}_0 \in \mathcal{N}. \end{cases} \quad (3.5)$$

If \mathbf{x}_0 is not a vertex of the triangulation, an additional term h_{K_0} appears in the indicators corresponding to the triangle $\mathbf{x}_0 \in \bar{K}_0$.

To derive the reliability bound of a posteriori error estimator, we introduce the linear operator E_h mapping elements in $V_{h,0}^m$ onto a C^1 conforming macro-elements space S_h^{m+2} of degree $m+2$. For the detailed definition of this C^1 conforming macro-elements, refer to [22, 16]. For the convenience of readers, we provide a brief review of the high-order versions of the classical Hsieh-Clough-Tocher macro-element.

Definition 3.1 ([22]). Let element $K \in \mathcal{T}_h$. For $m \geq 2$, a macro-element of degree $m+2$ is a nodal finite element $(K, \tilde{P}_{m+2}, \tilde{N}_{m+2})$. Here, the element K consists of subtriangles K_i , $i = 1, 2, 3$ satisfying $\bar{K} = \cup_{i=1}^3 \bar{K}_i$ as shown in Figure 3(b). The local element space \tilde{P}_{m+2} on K is defined by

$$\tilde{P}_{m+2} := \{v \in C^1(K) : v|_{K_i} \in P_{m+2}(K_i), i = 1, 2, 3\}. \quad (3.6)$$

The degrees of freedom \tilde{N}_{m+2} on K consist of all the following values:

- The value and the first (partial) derivatives at the vertices of K ;
- The value at $m-1$ distinct points in the interior of each exterior edge of K ;
- The normal derivative at m distinct points in the interior of each exterior edge of K ;
- The value and the first (partial) derivatives at the common vertex of all K_i , where $i = 1, 2, 3$;
- The value and the normal derivative at $m-2$ distinct points in the interior of each edge of the K_i , where $i = 1, 2, 3$, that is not an edge of K ;
- The value at $(m-2)(m-3)/2$ distinct points in the interior of each K_i chosen so that, if a polynomial of degree $m-4$ vanishes at those points, then it vanishes identically.

For example, the \tilde{P}_5 macro-element is a C^1 extension of the C^0 Lagrange element that consists of P_3 polynomials. These elements are illustrated in Figure 3, where we use the solid dot (\bullet) to denote the value of the shape functions, the circle (\circ) to denote the value of all the first (partial) derivatives of the shape functions, and the arrow (\uparrow) to denote the value of the normal derivatives.

Denote by ω_v the set of elements containing a node $v \in \mathcal{N}$, and let $\#\omega_v$ denote the number of elements in ω_v . We construct E_h by averaging the nodal function values as follows:

$$N_v(E_h(u_h)) = \begin{cases} \frac{1}{\#\omega_v} \sum_{K \in \omega_v} N_v(u_h|_K), & \text{if } v \notin \partial\Omega; \\ 0, & \text{if } v \in \partial\Omega. \end{cases} \quad (3.7)$$

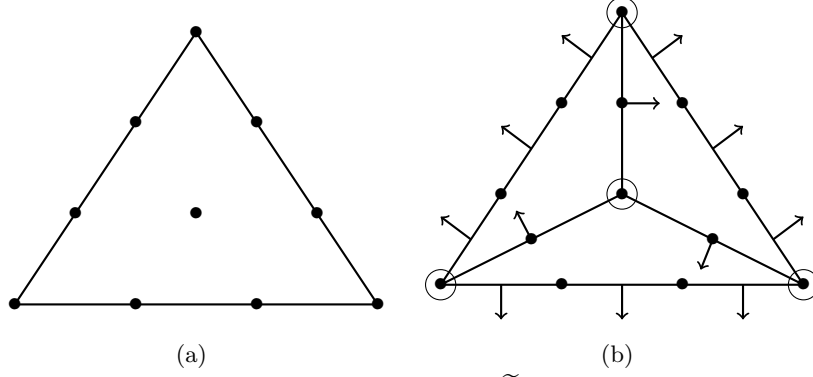


FIGURE 3. (a) A P_3 Lagrange element. (b) A \tilde{P}_5 C^1 conforming macro element.

Here, N_v represents either the nodal value of a shape function, its first partial derivatives, or its normal derivative at v , where v is any node in the macro-elements space S_h^{m+2} .

Lemma 3.1. [22, Lemma 2.9] Let $u_h \in V_{h,0}^m$ be the solution of (2.9). Then there exists an operator $E_h : V_{h,0}^m \rightarrow S_h^{m+2} \cap H_0^2(\Omega)$ that satisfies the following bound

$$\sum_{K \in \mathcal{T}_h} |u_h - E_h(u_h)|_{H^l(K)}^2 \leq C \sum_{e \in \mathcal{E}_h} h_e^{3-2l} \|[\nabla u_h]\|_{L^2(e)}^2, \quad l = 0, 1, 2. \quad (3.8)$$

Remark 3.2. Different from the estimate in [22], the right-hand side of (3.8) here does not include the term $\sum_{e \in \mathcal{E}_h} h_e^{1-2l} \|[[u_h]]\|_{L^2(e)}^2$. This is because $V_h^m \subset C^0(\Omega)$, then the jump of u_h across any edge $e \in \mathcal{E}_I$ is zero, and $u_h|_e = 0$ for $e \in \mathcal{E}_B$.

We further introduce the following result.

Lemma 3.3 (Weak continuity). Let u be the solution of the problem (1.1). Then for any $e \in \mathcal{E}_I$,

$$\int_e [[u]] \cdot \mathbf{q} \, ds = 0, \quad \forall \mathbf{q} \in [L^2(e)]^2, \quad (3.9)$$

$$\int_e [[\nabla u]] v \, ds = 0, \quad \forall v \in L^2(e), \quad (3.10)$$

$$\int_e [[\Delta u]] \cdot \mathbf{q} \, ds = 0, \quad \forall \mathbf{q} \in [L^2(e)]^2, \quad (3.11)$$

$$\int_e [[\nabla \Delta u]] v \, ds = 0, \quad \forall v \in L^2(e). \quad (3.12)$$

Proof. Given that $u \in H^{\min\{3-\epsilon, 2+\alpha\}}(\Omega) \cap H_0^2(\Omega)$, (3.9) and (3.10) follow immediately. We denote the set of the neighborhoods of the domain corners by Ω_C and of the singular point \mathbf{x}_0 by $\Omega_{\mathbf{x}_0}$. Then $u \in H^4(\Omega \setminus (\Omega_C \cup \Omega_{\mathbf{x}_0}))$. Therefore, (3.11) and (3.12) hold for any $e \in \Omega \setminus (\Omega_C \cup \Omega_{\mathbf{x}_0})$. To this end, we show that they also hold for $e \in \Omega_C \cup \Omega_{\mathbf{x}_0}$. In the neighborhood of \mathbf{x}_0 , the solution u can be decomposed as $u = u_R + u_{\mathbf{x}_0}$, where $u_R \in H^4(\Omega_{\mathbf{x}_0})$ and $u_{\mathbf{x}_0} = -\frac{|\mathbf{x} - \mathbf{x}_0|}{8\pi} \ln |\mathbf{x} - \mathbf{x}_0|$ is the fundamental solution of the biharmonic equation with the Dirac delta function $\delta_{\mathbf{x}_0}$. It is straightforward to verify that (3.11) and (3.12) hold for any $e \in \Omega_{\mathbf{x}_0}$, and they can be similarly proved for any $e \in \Omega_C$. \square

Let ω_e be the collection of two adjacent elements that share the common edge e . Specially, we define

$$\omega_e^0 = \{K \in \mathcal{T}_h : \partial K \cap \partial K_0 = e\}.$$

For any $K \in \omega_e$, by (2.5) and the shape regular assumption, there exist positive constants C_1 and C_2 such that

$$C_1 h_K \leq h_e \leq C_2 h_K.$$

Next, we are ready to present one of the main results.

Theorem 3.4 (Reliability). Let u be the solution of (1.1) and $u_h \in V_{h,0}^m$ be the solution of (2.9). Then the residual-based a posteriori error estimator η satisfies the global bound

$$|||u - u_h||| \leq C\eta. \quad (3.13)$$

Proof. Recall the energy norm $||| \cdot |||$ in (2.11). It follows

$$|||u - u_h|||^2 = \sum_{K \in \mathcal{T}_h} |u - u_h|_{H^2(K)}^2 + \sum_{e \in \mathcal{E}_h} \frac{\beta}{h_e} \|[\![\nabla(u - u_h)]\!] \|_{L^2(e)}^2.$$

According to the Lemma 3.3, it is clearly that

$$\|[\![\nabla(u - u_h)]\!] \|_{L^2(e)}^2 = \int_e [|\nabla u|^2 - 2[\![\nabla u][\![\nabla u_h]] + |\nabla u_h|^2] ds = \int_e [|\nabla u_h|^2] ds = \|[\![\nabla u_h]] \|_{L^2(e)}^2,$$

then

$$\sum_{e \in \mathcal{E}_h} \frac{\beta}{h_e} \|[\![\nabla(u - u_h)]\!] \|_{L^2(e)}^2 = \sum_{e \in \mathcal{E}_h} \frac{\beta}{h_e} \|[\![\nabla u_h]] \|_{L^2(e)}^2 \leq C \sum_{e \in \mathcal{E}_h} \eta_{2,e}^2.$$

Let $\chi = E_h u_h \in H_0^2(\Omega)$, the triangle inequality gives

$$\sum_{K \in \mathcal{T}_h} |u - u_h|_{H^2(K)}^2 \leq \sum_{K \in \mathcal{T}_h} |\chi - u_h|_{H^2(K)}^2 + \sum_{K \in \mathcal{T}_h} |u - \chi|_{H^2(K)}^2. \quad (3.14)$$

By Lemma 3.1, it holds

$$\sum_{K \in \mathcal{T}_h} |\chi - u_h|_{H^2(K)}^2 \leq C \sum_{e \in \mathcal{E}_h} \eta_{2,e}^2.$$

To this end, it suffices to show that the second term on the right-hand side of (3.14) satisfies

$$\left(\sum_{K \in \mathcal{T}_h} |u - \chi|_{H^2(K)}^2 \right)^{1/2} \leq C\eta. \quad (3.15)$$

By (2.12) and duality argument,

$$\left(\sum_{K \in \mathcal{T}_h} |u - \chi|_{H^2(K)}^2 \right)^{1/2} = |u - \chi|_{H^2(\Omega)} \leq \sup_{\phi \in H_0^2(\Omega) \setminus \{0\}} \frac{a(u - \chi, \phi)}{|\phi|_{H^2(\Omega)}}. \quad (3.16)$$

Denote the continuous interpolation polynomial of ϕ by $\phi_I = \Pi_h \phi \in V_{h,0}^m$. By (2.12), (2.1) and (2.9),

$$\begin{aligned} a(u - \chi, \phi) &= a(u, \phi) + a_h(u_h, \phi) - a(\chi, \phi) - a_h(u_h, \phi) \\ &= a(u, \phi) + a_h(u_h - \chi, \phi) - a_h(u_h, \phi) \\ &= \langle \delta_{\mathbf{x}_0}, \phi \rangle + a_h(u_h - \chi, \phi) - a_h(u_h, \phi_I) - a_h(u_h, \phi - \phi_I) \\ &= \langle \delta_{\mathbf{x}_0}, \phi \rangle - A_h(u_h, \phi_I) + a_h(u_h - \chi, \phi) + A_h(u_h, \phi_I) - a_h(u_h, \phi_I) - a_h(u_h, \phi - \phi_I) \\ &= \langle \delta_{\mathbf{x}_0}, \phi - \phi_I \rangle + a_h(u_h - \chi, \phi) + A_h(u_h, \phi_I) - a_h(u_h, \phi_I) - a_h(u_h, \phi - \phi_I). \end{aligned} \quad (3.17)$$

To estimate the first term on the right-hand side of (3.17), we consider the following three possibilities based on the different locations of \mathbf{x}_0 . Recall that \mathcal{N} is the set of all mesh nodes of the triangulation.

(1) If $\mathbf{x}_0 \in \mathcal{N}$, the values of ϕ_I and ϕ are equal at the node \mathbf{x}_0 , i.e., $\phi(\mathbf{x}_0) = \phi_I(\mathbf{x}_0)$, then

$$\langle \delta_{\mathbf{x}_0}, \phi - \phi_I \rangle = \phi(\mathbf{x}_0) - \phi_I(\mathbf{x}_0) = 0. \quad (3.18)$$

(2) If $\mathbf{x}_0 \notin \mathcal{N}$, but it is located inside one element $K_0 \in \mathcal{T}_h$, it follows

$$\langle \delta_{\mathbf{x}_0}, \phi - \phi_h \rangle \leq \|\phi - \phi_I\|_{L^\infty(K_0)} \leq Ch_{K_0} |\phi|_{H^2(K_0)} \leq Ch_{K_0} |\phi|_{H^2(\Omega)}. \quad (3.19)$$

(3) If $\mathbf{x}_0 \notin \mathcal{N}$, but it belongs to an internal edge e , then

$$\langle \delta_{\mathbf{x}_0}, \phi - \phi_I \rangle \leq \|\phi - \phi_I\|_{L^\infty(\omega_e)} \leq Ch_{K_0} |\phi|_{H^2(\omega_e)} \leq Ch_{K_0} |\phi|_{H^2(\Omega)}. \quad (3.20)$$

By the Cauchy-Schwarz inequality and Lemma 3.1, the second term in (3.17) follows

$$a_h(u_h - \chi, \phi) \leq \left(\sum_{K \in \mathcal{T}_h} |u_h - \chi|_{H^2(K)}^2 \right)^{1/2} |\phi|_{H^2(\Omega)} \leq C \left(\sum_{e \in \mathcal{E}_h} \eta_{2,e}^2 \right)^{1/2} |\phi|_{H^2(\Omega)}. \quad (3.21)$$

According to the definition of $A_h(\cdot, \cdot)$ and $a_h(\cdot, \cdot)$, it is clear that

$$A_h(u_h, \phi_I) - a_h(u_h, \phi_I) = - \sum_{e \in \mathcal{E}_h} \int_e \{ \{ \Delta u_h \} \} [\nabla \phi_I] ds - \sum_{e \in \mathcal{E}_h} \int_e [\nabla u_h] \{ \{ \Delta \phi_I \} \} ds + \sum_{e \in \mathcal{E}_h} \frac{\beta}{h_e} \int_e [\nabla u_h] [\nabla \phi_I] ds.$$

Recall that $\phi \in H_0^2(\Omega)$, $\phi_I \in V_{h,0}^m$. Then $\phi - \phi_I$ is continuous, and $(\phi - \phi_I)|_e = 0$ for any $e \in \mathcal{E}_B$. By Lemma 3.3, it holds $\int_e [\nabla \phi] v ds = 0$, $\forall v \in L^2(e)$ for any $e \in \mathcal{E}_I$. Therefore,

$$\sum_{K \in \mathcal{T}_h} \int_{\partial K} \nabla(\Delta u_h) \cdot \mathbf{n}(\phi - \phi_I) ds = \sum_{e \in \mathcal{E}_I} \int_e [\nabla(\Delta u_h)](\phi - \phi_I) ds,$$

which together with the integration by parts, and (2.8) yields

$$\begin{aligned} -a_h(u_h, \phi - \phi_I) &= - \sum_{K \in \mathcal{T}_h} \int_K \Delta u_h \Delta(\phi - \phi_I) d\mathbf{x} \\ &= \sum_{K \in \mathcal{T}_h} \left(\int_K \nabla(\Delta u_h) \cdot \nabla(\phi - \phi_I) d\mathbf{x} - \int_{\partial K} \Delta u_h \nabla(\phi - \phi_I) \cdot \mathbf{n} ds \right) \\ &= - \sum_{K \in \mathcal{T}_h} \left(\int_K \Delta^2 u_h (\phi - \phi_I) d\mathbf{x} + \int_{\partial K} \nabla(\Delta u_h) \cdot \mathbf{n}(\phi - \phi_I) ds - \int_{\partial K} \Delta u_h \nabla(\phi - \phi_I) \cdot \mathbf{n} ds \right) \\ &= - \sum_{K \in \mathcal{T}_h} \int_K \Delta^2 u_h (\phi - \phi_I) d\mathbf{x} + \sum_{e \in \mathcal{E}_I} \int_e [\nabla(\Delta u_h)](\phi - \phi_I) ds \\ &\quad - \sum_{e \in \mathcal{E}_I} \int_e [\Delta u_h] \cdot \{ \{ \nabla(\phi - \phi_I) \} \} ds + \sum_{e \in \mathcal{E}_h} \int_e \{ \{ \Delta u_h \} \} [\nabla \phi_I] ds. \end{aligned}$$

The sum of the two qualities above gives

$$\begin{aligned} &(A_h(u_h, \phi_I) - a_h(u_h, \phi_I)) - a_h(u_h, \phi - \phi_I) \\ &= - \sum_{K \in \mathcal{T}_h} \int_K \Delta^2 u_h (\phi - \phi_I) d\mathbf{x} + \sum_{e \in \mathcal{E}_I} \int_e [\nabla(\Delta u_h)](\phi - \phi_I) ds \\ &\quad - \sum_{e \in \mathcal{E}_I} \int_e [\Delta u_h] \cdot \{ \{ \nabla(\phi - \phi_I) \} \} ds - \sum_{e \in \mathcal{E}_h} \int_e [\nabla u_h] \{ \{ \Delta \phi_I \} \} ds + \sum_{e \in \mathcal{E}_h} \frac{\beta}{h_e} \int_e [\nabla u_h] [\nabla \phi_I] ds. \end{aligned}$$

Then, we estimate the five terms on the right hand side of the above equation one by one. Using the Cauchy-Schwarz inequality and Lemma 2.6 gives

$$\begin{aligned} \sum_{K \in \mathcal{T}_h} \int_K \Delta^2 u_h (\phi - \phi_I) \, d\mathbf{x} &\leq \sum_{K \in \mathcal{T}_h} \|\Delta^2 u_h\|_{L^2(K)} \|\phi - \phi_I\|_{L^2(K)} \leq C \sum_{K \in \mathcal{T}_h} h_K^2 \|\Delta^2 u_h\|_{L^2(K)} |\phi|_{H^2(K)} \\ &\leq C \left(\sum_{K \in \mathcal{T}_h} \eta_{1,K}^2 \right)^{1/2} |\phi|_{H^2(\Omega)}, \end{aligned} \quad (3.22)$$

$$\begin{aligned} \sum_{e \in \mathcal{E}_I} \int_e \llbracket \nabla(\Delta u_h) \rrbracket (\phi - \phi_I) \, ds &\leq \left(\sum_{e \in \mathcal{E}_I} h_e^3 \int_e \llbracket \nabla(\Delta u_h) \rrbracket^2 \, ds \right)^{1/2} \left(\sum_{e \in \mathcal{E}_I} h_e^{-3} \int_e (\phi - \phi_I)^2 \, ds \right)^{1/2} \\ &\leq C \left(\sum_{e \in \mathcal{E}_I} \eta_{4,e}^2 \right)^{1/2} |\phi|_{H^2(\Omega)}, \end{aligned} \quad (3.23)$$

and

$$\begin{aligned} \sum_{e \in \mathcal{E}_h} \frac{\beta}{h_e} \int_e \llbracket \nabla u_h \rrbracket \llbracket \nabla \phi_I \rrbracket \, ds &\leq \left(\sum_{e \in \mathcal{E}_h} \int_e \beta^2 h_e^{-1} \llbracket \nabla u_h \rrbracket^2 \, ds \right)^{1/2} \left(\sum_{e \in \mathcal{E}_h} h_e^{-1} \int_e \llbracket \nabla \phi_I \rrbracket^2 \, ds \right)^{1/2} \\ &= \left(\sum_{e \in \mathcal{E}_h} \int_e \beta^2 h_e^{-1} \llbracket \nabla u_h \rrbracket^2 \, ds \right)^{1/2} \left(\sum_{e \in \mathcal{E}_h} h_e^{-1} \int_e \llbracket \nabla(\phi - \phi_I) \rrbracket^2 \, ds \right)^{1/2} \\ &\leq C \left(\sum_{e \in \mathcal{E}_h} \eta_{2,e}^2 \right)^{1/2} |\phi|_{H^2(\Omega)}. \end{aligned} \quad (3.24)$$

For any $e = \partial K^+ \cap \partial K^- \in \mathcal{E}_I$, applying Lemma 2.6 and Lemma 2.5 gives

$$\begin{aligned} \|\llbracket \nabla(\phi - \phi_I) \rrbracket\|_{L^2(e)} &\leq \frac{1}{2} (\|\nabla(\phi - \phi_I)|_{K^+}\|_{L^2(e)} + \|\nabla(\phi - \phi_I)|_{K^-}\|_{L^2(e)}) \\ &\leq C (\|\nabla(\phi - \phi_I)\|_{L^2(\partial K^+)} + \|\nabla(\phi - \phi_I)\|_{L^2(\partial K^-)}) \\ &\leq C (h_{K^+}^{1/2} |\phi|_{H^2(K^+)} + h_{K^-}^{1/2} |\phi|_{H^2(K^-)}), \end{aligned}$$

$$\begin{aligned} \|\llbracket \Delta \phi_I \rrbracket\|_{L^2(e)} &\leq \frac{1}{2} (\|\Delta \phi_I|_{K^+}\|_{L^2(e)} + \|\Delta \phi_I|_{K^-}\|_{L^2(e)}) \\ &\leq C (h_{K^+}^{-1/2} \|\Delta \phi_I\|_{L^2(K^+)} + h_{K^-}^{-1/2} \|\Delta \phi_I\|_{L^2(K^-)}) \\ &\leq C [h_{K^+}^{-1/2} (\|\Delta(\phi_I - \phi)\|_{L^2(K^+)} + \|\Delta \phi\|_{L^2(K^+)}) \\ &\quad + h_{K^-}^{-1/2} (\|\Delta(\phi_I - \phi)\|_{L^2(K^-)} + \|\Delta \phi\|_{L^2(K^-)})] \\ &\leq C (h_{K^+}^{-1/2} |\phi|_{H^2(K^+)} + h_{K^-}^{-1/2} |\phi|_{H^2(K^-)}). \end{aligned}$$

Recall that h_e is equivalent to h_{K^+} and h_{K^-} . Summing up over all interior edges $e \in \mathcal{E}_I$ leads to

$$\begin{aligned} \sum_{e \in \mathcal{E}_I} h_e^{-1} \|\{\{\nabla(\phi - \phi_I)\}\}\|_{L^2(e)}^2 &\leq C \sum_{e \in \mathcal{E}_I} h_e^{-1} \left(h_{K^+}^{1/2} |\phi|_{H^2(K^+)} + h_{K^-}^{1/2} |\phi|_{H^2(K^-)} \right)^2 \\ &\leq C \sum_{e \in \mathcal{E}_I} h_e^{-1} \left(h_{K^+} |\phi|_{H^2(K^+)}^2 + h_{K^-} |\phi|_{H^2(K^-)}^2 \right) \\ &\leq C |\phi|_{H^2(\Omega)}^2, \end{aligned}$$

$$\begin{aligned} \sum_{e \in \mathcal{E}_I} h_e \|\{\{\Delta\phi_I\}\}\|_{L^2(e)}^2 &\leq C \sum_{e \in \mathcal{E}_I} h_e \left(h_{K^+}^{-1/2} |\phi|_{H^2(K^+)} + h_{K^-}^{-1/2} |\phi|_{H^2(K^-)} \right)^2 \\ &\leq C \sum_{e \in \mathcal{E}_I} h_e \left(h_{K^+}^{-1} |\phi|_{H^2(K^+)}^2 + h_{K^-}^{-1} |\phi|_{H^2(K^-)}^2 \right) \\ &\leq C |\phi|_{H^2(\Omega)}^2. \end{aligned}$$

Similarly, for any $e \in \partial K \cap \mathcal{E}_B$, applying Lemma 2.6 and Lemma 2.5 gives

$$\sum_{e \in \mathcal{E}_B} h_e \|\{\{\Delta\phi_I\}\}\|_{L^2(e)}^2 \leq C |\phi|_{H^2(\Omega)}^2$$

Then, by using the Cauchy-Schwarz inequality, it holds

$$\begin{aligned} \sum_{e \in \mathcal{E}_I} \int_e \llbracket \Delta u_h \rrbracket \cdot \{\{\nabla(\phi - \phi_I)\}\} ds &\leq \left(\sum_{e \in \mathcal{E}_I} h_e \int_e \llbracket \Delta u_h \rrbracket^2 ds \right)^{1/2} \left(\sum_{e \in \mathcal{E}_I} h_e^{-1} \int_e \{\{\nabla(\phi - \phi_I)\}\}^2 ds \right)^{1/2} \\ &\leq C \left(\sum_{e \in \mathcal{E}_I} \eta_{3,e}^2 \right)^{1/2} |\phi|_{H^2(\Omega)}, \end{aligned} \quad (3.25)$$

$$\begin{aligned} \sum_{e \in \mathcal{E}_h} \int_e \llbracket \nabla u_h \rrbracket \{\{\Delta\phi_I\}\} ds &\leq \left(\sum_{e \in \mathcal{E}_h} h_e^{-1} \int_e \llbracket \nabla u_h \rrbracket^2 ds \right)^{1/2} \left(\sum_{e \in \mathcal{E}_h} h_e \int_e \{\{\Delta\phi_I\}\}^2 ds \right)^{1/2} \\ &\leq C \left(\sum_{e \in \mathcal{E}_h} \eta_{2,e}^2 \right)^{1/2} |\phi|_{H^2(\Omega)}. \end{aligned} \quad (3.26)$$

The estimates (3.18) - (3.26) imply that (3.15) holds. □

To prove the efficiency of the a posteriori error estimator, we will define four types of “bubble” functions and introduce some properties of these functions that are frequently used in error estimation and analysis. Let \hat{K} be a reference triangular or rectangular element. If \hat{K} is a triangle with the barycentric coordinates λ_1, λ_2 and λ_3 , we denote the standard “bubble” function in \hat{K} by

$$b_{\hat{K}} = 27\lambda_1\lambda_2\lambda_3. \quad (3.27)$$

If \hat{K} is a rectangle with the corresponding coordinates x and y , we denote the “bubble” function in \hat{K} by

$$b_{\hat{K}} = (1 - x^2)(1 - y^2). \quad (3.28)$$

For a triangle $K \in \mathcal{T}_h$, we define $F_K : \hat{K} \rightarrow K$ as an affine element mapping, where \hat{K} is the reference triangle. Then the “bubble” function b_K on K is defined as

$$b_K = \begin{cases} b_{\hat{K}} \circ F_K, & \text{if } K \in \mathcal{T}_h \setminus K_0, \\ \frac{|\mathbf{x} - \mathbf{x}_0|^2}{h_{K_0}^2} b_{\hat{K}} \circ F_{K_0}, & \text{if } K = K_0. \end{cases} \quad (3.29)$$

Lemma 3.5. For the element “bubble” function b_K on a triangle $K \in \mathcal{T}_h$, it holds

$$b_K(\mathbf{x}_0) = 0, \quad b_K(\mathbf{x}) = 0, \quad \forall \mathbf{x} \in \Omega \setminus K. \quad (3.30)$$

Moreover, for $\forall v \in P_m(K)$, it follows

$$\|v\|_{L^2(K)} \leq C \|b_K v\|_{L^2(K)}, \quad \|b_K^2 v\|_{L^2(K)} \leq C \|v\|_{L^2(K)}. \quad (3.31)$$

For each internal edge $e \in \mathcal{E}_I$, let $T \subset \omega_e$ be the largest rhombus contained in ω_e that has e as one of its diagonals. We define $F_T : \hat{K} \rightarrow T$ as an affine element mapping, where \hat{K} is the reference rectangle. The “bubble” function b_T on element T is defined by

$$b_T = \begin{cases} b_{\hat{K}} \circ F_T, & \text{if } \mathbf{x}_0 \notin \bar{T}, \\ \frac{|\mathbf{x} - \mathbf{x}_0|^2}{h_e^2} b_{\hat{K}} \circ F_T, & \text{if } \mathbf{x}_0 \in \bar{T}, \end{cases} \quad (3.32)$$

where \bar{T} is the closure of T .

Lemma 3.6. For the “bubble” function b_T in rhombus T , it holds

$$b_T^3 \in C^2(\Omega) \cap H_0^2(\Omega), \quad b_T(\mathbf{x}_0) = 0, \quad \{\{b_T^3\}\} = 0 \quad \text{on } \mathcal{E}_h \setminus e, \quad (3.33)$$

$$\llbracket b_T^3 \rrbracket = \mathbf{0} \quad \text{and} \quad \llbracket \nabla b_T^3 \rrbracket = \{\{\nabla b_T^3\}\} \cdot \mathbf{n} = 0 \quad \text{on } \mathcal{E}_h. \quad (3.34)$$

Moreover, for $\forall v \in P_m(K)$, it follows

$$\|v\|_{L^2(e)} \leq C \|b_T^{3/2} v\|_{L^2(e)}, \quad \|v b_T^3\|_{L^2(\omega_e)} \leq h_e^{1/2} \|v\|_{L^2(e)}. \quad (3.35)$$

Remark 3.7. Inspired by the “bubble” functions in [20], where it is used to estimate the a posterior estimator of the discontinuous Galerkin method for the fourth-order elliptic problem with a source term in $L^2(\Omega)$. Here we modify the definition of “bubble” functions b_K and b_T to accommodate two specific cases. Compared to [20], we further consider the effects of singularity point \mathbf{x}_0 . As a result, the new “bubble” functions retain the favorable properties of the original ones and also obtain values of 0 at \mathbf{x}_0 , which is crucial for the subsequent proof of lower bounds.

Let b_l be an affine function that satisfies $b_l|_e = 0$ and $(\nabla b_l \cdot \mathbf{n})|_e = h_e^{-1}$, where \mathbf{n} is the unit normal to the edge e . Using the element “bubble” function definition given above, we define an edge “bubble” function as

$$b_e = b_l b_T^3. \quad (3.36)$$

Lemma 3.8. For the edge “bubble” function b_e in (3.36), it holds

$$b_e \in C^2(\Omega) \cap H_0^2(\Omega), \quad b_e(\mathbf{x}_0) = 0, \quad b_e = 0 \quad \text{in } \Omega \setminus T, \quad (3.37)$$

$$\llbracket b_e \rrbracket = \mathbf{0} \quad \text{and} \quad \llbracket \nabla b_e \rrbracket = \{\{b_e\}\} = 0 \quad \text{on } \mathcal{E}_h, \quad (3.38)$$

$$(\{\{\nabla b_e\}\} \cdot \mathbf{n})|_e = h_e^{-1} b_T^3|_e, \quad \{\{\nabla b_e\}\} = \mathbf{0} \quad \text{on } \mathcal{E}_h \setminus e, \quad (3.39)$$

Moreover, for $\forall v \in P_m(K)$, it follows

$$\|b_e v\|_{L^2(\omega_e)} \leq C h_e^{1/2} \|v\|_{L^2(e)}. \quad (3.40)$$

Denote ω_K by the collection of elements in \mathcal{T}_h that share a common edge or vertex with K . Specially, we define the set

$$\omega_{K_0} = \{K \in \mathcal{T}_h : \bar{K} \cap \bar{K}_0 \neq \emptyset\}, \quad (3.41)$$

and the distance of \mathbf{x}_0 to the boundary of ω_{K_0} is defined by $d := \text{dist}(\mathbf{x}_0, \partial\omega_{K_0})$. We define the smooth “bubble” function associated with the point \mathbf{x}_0 by convolution of the characteristic function of the set $\{\mathbf{x} \in \Omega : |\mathbf{x} - \mathbf{x}_0| < d/4\}$ satisfying

$$\begin{aligned} 0 \leq b_{\mathbf{x}_0}(\mathbf{x}) \leq 1, \quad \forall \mathbf{x} \in \Omega, \quad |b_{\mathbf{x}_0}(\mathbf{x})|_{m, \infty, \omega_{K_0}} &\leq Cd^{-m}, \quad m = 1, 2, \\ b_{\mathbf{x}_0}(\mathbf{x}) &= 1, \quad \forall \mathbf{x} \in \Omega : |\mathbf{x} - \mathbf{x}_0| \leq \frac{d}{4}, \\ b_{\mathbf{x}_0}(\mathbf{x}) &= 0, \quad \forall \mathbf{x} \in \Omega : |\mathbf{x} - \mathbf{x}_0| \geq \frac{3d}{4}. \end{aligned}$$

Lemma 3.9. Assume that $\mathbf{x}_0 \in \bar{K}_0$. For the “bubble” function $b_{\mathbf{x}_0}$, it holds,

$$|b_{\mathbf{x}_0}(\mathbf{x})|_{H^m(\omega_{K_0})} \leq Ch_{K_0}^{1-m}, \quad m = 0, 1, 2. \quad (3.42)$$

$$\|b_{\mathbf{x}_0}(\mathbf{x})\|_{L^2(e)} \leq Ch_e^{1/2}, \quad e \in \partial\omega_{K_0}. \quad (3.43)$$

Proof. The proof of (3.42) follow from Lemma 3.2 [1]. For (3.43), the definition of $\|\cdot\|_{L^2(e)}$ yields

$$\|b_{\mathbf{x}_0}(\mathbf{x})\|_{L^2(e)} = \left(\int_e b_{\mathbf{x}_0}^2(s) ds \right)^{1/2} \leq C \left(\int_e ds \right)^{1/2} = Ch_e^{1/2}.$$

□

Then we are ready to present our next main result.

Theorem 3.10 (Efficiency). For the local indicator η_K defined in (3.1), there exists a positive constant C independent of the mesh size satisfying

$$\eta_K \leq C \| \|u - u_h\| \|_{\omega_K}. \quad (3.44)$$

Proof. We first prove the estimate (3.44) on the element \bar{K}_0 whose closure contains \mathbf{x}_0 , but $\mathbf{x}_0 \notin \mathcal{N}$. By the definition of the energy norm, it holds

$$\| \|u - u_h\| \|_{\omega_{K_0}}^2 = \sum_{K \in \omega_{K_0}} \left(|u - u_h|_{H^2(K)}^2 + \sum_{e \in \mathcal{E}_K} \frac{\beta}{h_e} \| [\nabla(u - u_h)] \|_{L^2(e)}^2 \right),$$

the estimation (3.44) is equivalent to

$$\left(h_{K_0}^2 + \eta_{1, K_0}^2 + \sum_{e \in \mathcal{E}_{K_0} \cap \mathcal{E}_I} \alpha_e \eta_{3, e}^2 + \sum_{e \in \mathcal{E}_{K_0} \cap \mathcal{E}_I} \alpha_e \eta_{4, e}^2 \right)^{1/2} \leq C \| \|u - u_h\| \|_{\omega_{K_0}}. \quad (3.45)$$

Then, we prove (3.45) in four steps.

(i) To prove $\eta_{1, K_0} = h_{K_0}^2 \|\Delta^2 u_h\|_{L^2(K_0)} \leq C \| \|u - u_h\| \|_{\omega_{K_0}}$. For $\forall v \in V_{h, 0}^m$, using integration by part gives

$$\begin{aligned} v(\mathbf{x}_0) - \int_{K_0} (\Delta^2 u_h) v \, d\mathbf{x} &= \int_{K_0} \Delta^2(u - u_h) v \, d\mathbf{x} \\ &= - \int_{K_0} \nabla \Delta(u - u_h) \cdot \nabla v \, d\mathbf{x} + \int_{\partial K_0} \nabla \Delta(u - u_h) \cdot \mathbf{n} v \, ds \\ &= \int_{K_0} \Delta(u - u_h) \Delta v \, d\mathbf{x} - \int_{\partial K_0} \Delta(u - u_h) \mathbf{n} \cdot \nabla v \, ds + \int_{\partial K_0} \nabla \Delta(u - u_h) \cdot \mathbf{n} v \, ds. \end{aligned} \quad (3.46)$$

We set $v|_{K_0} = (\Delta^2 u_h) b_{K_0}^2$ in (3.46), where $v \in H_0^2(\Omega) \cap H_0^2(K_0)$ and satisfies $v = 0$ in $\Omega \setminus K_0$. Additionally, v is a polynomial on K with $b_{K_0}(\mathbf{x}_0) = 0$. Then, for $\forall e \in \partial K_0$, it holds that $v(\mathbf{x}_0) = v|_e = \nabla v|_e = 0$. Consequently, (3.46) yields

$$\int_{K_0} \Delta(u - u_h) \Delta v \, d\mathbf{x} = - \int_{K_0} \Delta^2 u_h v \, d\mathbf{x}.$$

According to Lemma 3.5, it holds

$$\|v\|_{L^2(K_0)} \leq C \|\Delta^2 u_h\|_{L^2(K_0)}.$$

Then, by Cauchy-Schwarz inequality and Lemma 2.5,

$$\begin{aligned} \int_{K_0} (\Delta^2 u_h) v \, d\mathbf{x} &\leq \|\Delta(u - u_h)\|_{L^2(K_0)} \|v\|_{H^2(K_0)} \leq Ch_{K_0}^{-2} |u - u_h|_{H^2(\omega_{K_0})} \|v\|_{L^2(K_0)} \\ &\leq Ch_{K_0}^{-2} |u - u_h|_{H^2(\omega_{\mathbf{x}_0})} \|\Delta^2 u_h\|_{L^2(K_0)}. \end{aligned} \quad (3.47)$$

Since $\Delta^2 u_h$ is a piecewise polynomial over K_0 , according to (3.31) and (3.47), it holds

$$\begin{aligned} \|\Delta^2 u_h\|_{L^2(K_0)}^2 &\leq C \int_{K_0} (\Delta^2 u_h)^2 b_{K_0}^2 \, d\mathbf{x} = C \int_{K_0} (\Delta^2 u_h) v \, d\mathbf{x} \\ &\leq Ch_{K_0}^{-2} |u - u_h|_{H^2(\omega_{K_0})} \|\Delta^2 u_h\|_{L^2(K_0)}, \end{aligned}$$

which implies

$$h_{K_0}^2 \|\Delta^2 u_h\|_{L^2(K_0)} \leq C |u - u_h|_{H^2(\omega_{K_0})} \leq C \| |u - u_h| \|_{\omega_{K_0}}. \quad (3.48)$$

(ii) To prove $\sum_{e \in \mathcal{E}_{K_0} \cap \mathcal{E}_I} \alpha_e \eta_{3,e}^2 = \sum_{e \in \mathcal{E}_{K_0}} h_e^{1/2} \|\llbracket \Delta u_h \rrbracket\|_{L^2(e)} \leq C \| |u - u_h| \|_{\omega_{K_0}}$. For $\forall e \in \mathcal{E}_{K_0} \cap \mathcal{E}_I$, denote by $\mathcal{F}_e = \{e \in \partial K : K \in \omega_e^0\}$. By (2.7), the summation of (3.46) over all elements $K \in \omega_e^0$ gives

$$\begin{aligned} v(\mathbf{x}_0) - \sum_{K \in \omega_e^0} \int_K \Delta^2 u_h v \, d\mathbf{x} &= \int_{\omega_e^0} \Delta(u - u_h) \Delta v \, d\mathbf{x} + \sum_{e \in \mathcal{F}_e \cap \mathcal{E}_I} \int_e \llbracket v \rrbracket \cdot \{\{\nabla \Delta(u - u_h)\}\} \, ds \\ &\quad + \sum_{e \in \mathcal{F}_e} \int_e \{\{v\}\} \llbracket \nabla \Delta(u - u_h) \rrbracket \, ds - \sum_{e \in \mathcal{F}_e} \int_e \llbracket \nabla v \rrbracket \{\{\Delta(u - u_h)\}\} \, ds \\ &\quad - \sum_{e \in \mathcal{F}_e \cap \mathcal{E}_I} \int_e \{\{\nabla v\}\} \cdot \llbracket \Delta(u - u_h) \rrbracket \, ds. \end{aligned} \quad (3.49)$$

We take $v = \phi b_e$ in (3.49), where ϕ is continuous on $e \in \mathcal{E}_h$, and ϕ is a constant function in the normal direction to e (i.e., $(\nabla \phi \cdot \mathbf{n})|_e = 0$). By $v(\mathbf{x}_0) = 0$, Lemma 3.3, and Lemma 3.8, the equality (3.49) reduces to

$$- \int_{\omega_e^0} \Delta^2 u_h v \, d\mathbf{x} = \int_e \{\{\nabla v\}\} \cdot \llbracket \Delta u_h \rrbracket \, ds + \int_{\omega_e^0} \Delta(u - u_h) \Delta v \, d\mathbf{x}.$$

By using Cauchy-Schwarz inequality and Lemma 2.5, the equation above gives

$$\begin{aligned} \int_e \llbracket \Delta u_h \rrbracket \cdot \{\{\nabla v\}\} \, ds &\leq \|\Delta^2 u_h\|_{L^2(\omega_e^0)} \|v\|_{L^2(\omega_e^0)} + |u - u_h|_{H^2(\omega_e^0)} \|\Delta v\|_{L^2(\omega_e^0)} \\ &\leq C (h_e^2 \|\Delta^2 u_h\|_{L^2(\omega_e^0)} + |u - u_h|_{H^2(\omega_e^0)}) h_e^{-2} \|v\|_{L^2(\omega_e^0)} \end{aligned} \quad (3.50)$$

We extend $(\llbracket \Delta u_h \rrbracket \cdot \mathbf{n})|_e$ from edge e to ω_e^0 by taking constants along the normal on e . The resulting extension $E(\llbracket \Delta u_h \rrbracket \cdot \mathbf{n})$ is a piecewise polynomial in ω_e . Setting $\phi = E(\llbracket \Delta u_h \rrbracket \cdot \mathbf{n})$, and using (3.35) and

(3.40) yield

$$\begin{aligned} \|\llbracket \Delta u_h \rrbracket\|_{L^2(e)}^2 &\leq C \int_e \llbracket \Delta u_h \rrbracket^2 b_T^3 \, ds = Ch_e \int_e \llbracket \Delta u_h \rrbracket \cdot \{\{\nabla v\}\} \, ds, \\ \|v\|_{L^2(\omega_e^0)} &\leq Ch_e^{1/2} \|\phi\|_{L^2(e)} = Ch_e^{1/2} \|\llbracket \Delta u_h \rrbracket\|_{L^2(e)}. \end{aligned} \quad (3.51)$$

By (3.48), (3.50)-(3.51), it follows

$$\begin{aligned} h_e^{1/2} \|\llbracket \Delta u_h \rrbracket\|_{L^2(e)}^2 &\leq Ch_e^{3/2} \int_e \llbracket \Delta u_h \rrbracket \cdot \{\{\nabla v\}\} \, ds \\ &\leq Ch_e^{-1/2} (h_e^2 \|\Delta^2 u_h\|_{L^2(\omega_e^0)} + |u - u_h|_{H^2(\omega_e^0)}) \|v\|_{L^2(\omega_e^0)} \\ &\leq C \| |u - u_h| \|_{\omega_e^0} \|\llbracket \Delta u_h \rrbracket\|_{L^2(e)}, \end{aligned}$$

which gives

$$h_e^{1/2} \|\llbracket \Delta u_h \rrbracket\|_{L^2(e)} \leq C \| |u - u_h| \|_{\omega_e^0}. \quad (3.52)$$

Summing up (3.52) over all edges $e \in \mathcal{E}_{K_0} \cap \mathcal{E}_I$ yields

$$\sum_{e \in \mathcal{E}_{K_0} \cap \mathcal{E}_I} h_e^{1/2} \|\llbracket \Delta u_h \rrbracket\|_{L^2(e)} \leq C \| |u - u_h| \|_{\omega_{K_0}}. \quad (3.53)$$

(iii) To prove $\sum_{e \in \mathcal{E}_{K_0} \cap \mathcal{E}_I} \alpha_e \eta_{4,e}^2 = \sum_{e \in \mathcal{E}_{K_0}} h_e^{3/2} \|\llbracket \nabla \Delta u_h \rrbracket\|_{L^2(e)} \leq C \| |u - u_h| \|_{\omega_{K_0}}$. We take $v = \Phi b_T^3$ in (3.49), where Φ is continuous on $e \in \mathcal{E}_h$ and $(\nabla \Phi \cdot \mathbf{n})|_e = 0$. By $b_T^3(\mathbf{x}_0) = 0$, Lemma 3.3, and Lemma 3.6, (3.49) can be written as

$$\int_{\omega_e^0} \Delta^2 u_h v \, dx + \int_{\omega_e^0} \Delta(u - u_h) \Delta v \, dx = \int_e \llbracket \nabla \Delta u_h \rrbracket \{\{v\}\} \, ds. \quad (3.54)$$

By (3.54), Cauchy-Schwarz inequality, and Lemma 2.5,

$$\int_e \llbracket \nabla \Delta u_h \rrbracket \{\{v\}\} \, ds \leq C (|u - u_h|_{H^2(\omega_e^0)} + h_e^2 \|\Delta^2 u_h\|_{L^2(\omega_e^0)}) h_e^{-2} \|v\|_{L^2(\omega_e^0)}. \quad (3.55)$$

We extend $(\llbracket \nabla \Delta u_h \rrbracket)|_e$ to a function $E(\llbracket \nabla \Delta u_h \rrbracket)$, defined over ω_e^0 , by taking it to be constants along lines normal to e . Setting $\Phi = E(\llbracket \nabla \Delta u_h \rrbracket)$ and using (3.35) yield

$$\begin{aligned} \|v\|_{L^2(\omega_e^0)} &\leq Ch_e^{1/2} \|\Phi\|_{L^2(e)} = Ch_e^{1/2} \|\llbracket \nabla \Delta u_h \rrbracket\|_{L^2(e)}, \\ \|\llbracket \nabla \Delta u_h \rrbracket\|_{L^2(e)}^2 &\leq C \int_e \llbracket \nabla \Delta u_h \rrbracket^2 b_T^3 \, ds = C \int_e \llbracket \nabla \Delta u_h \rrbracket \{\{v\}\} \, ds, \\ &\leq Ch_e^{-3/2} (|u - u_h|_{H^2(\omega_e^0)} + h_e^2 \|\Delta^2 u_h\|_{L^2(\omega_e^0)}) \|\llbracket \nabla \Delta u_h \rrbracket\|_{L^2(e)}. \end{aligned} \quad (3.56)$$

Form (3.48) and (3.55)-(3.56),

$$h_e^{3/2} \|\llbracket \nabla \Delta u_h \rrbracket\|_{L^2(e)} \leq C (h_e^2 \|\Delta^2 u_h\|_{L^2(\omega_e^0)} + |u - u_h|_{H^2(\omega_e^0)}) \leq C \| |u - u_h| \|_{\omega_e^0}, \quad (3.57)$$

Summing up (3.57) over all edges $e \in \mathcal{E}_{K_0} \cap \mathcal{E}_I$ gives

$$\sum_{e \in \mathcal{E}_{K_0} \cap \mathcal{E}_I} h_e^{3/2} \|\llbracket \nabla \Delta u_h \rrbracket\|_{L^2(e)} \leq C \| |u - u_h| \|_{\omega_{K_0}}. \quad (3.58)$$

(iv) To prove $h_{K_0} \leq C|||u - u_h|||_{\omega_{K_0}}$. By the weak formulation of (1.1) and Lemma 3.9, it can be observed

$$\begin{aligned}
1 &= \langle \delta_{\mathbf{x}_0}, b_{\mathbf{x}_0} \rangle \leq \left| \int_{\Omega} \Delta(u - u_h) \Delta b_{\mathbf{x}_0} \, d\mathbf{x} + \int_{\Omega} \Delta u_h \Delta b_{\mathbf{x}_0} \, d\mathbf{x} \right| \\
&\leq |u - u_h|_{H^2(\omega_{K_0})} |b_{\mathbf{x}_0}|_{H^2(\omega_{K_0})} + \left| \int_{\Omega} \Delta u_h \Delta b_{\mathbf{x}_0} \, d\mathbf{x} \right| \\
&\leq h_{K_0}^{-1} |u - u_h|_{H^2(\omega_{K_0})} + \left| \int_{\omega_{K_0}} \Delta u_h \Delta b_{\mathbf{x}_0} \, d\mathbf{x} \right|. \tag{3.59}
\end{aligned}$$

Let $\mathcal{F}_I = \{e \in \partial K \cap \mathcal{E}_I : K \in \omega_{K_0}\}$. By integration by parts, Cauchy-Schwarz inequality, Lemma 3.9 and Lemma 2.5,

$$\begin{aligned}
\int_{\omega_{K_0}} \Delta u_h \Delta b_{\mathbf{x}_0} \, d\mathbf{x} &= \sum_{K \in \omega_{K_0}} \int_K \Delta^2 u_h b_{\mathbf{x}_0} \, d\mathbf{x} - \int_{\partial K} \nabla(\Delta u_h) \cdot \mathbf{n} b_{\mathbf{x}_0} \, ds + \int_{\partial K} \Delta u_h \nabla b_{\mathbf{x}_0} \cdot \mathbf{n} \, ds \\
&= \sum_{K \in \omega_{K_0}} \int_K \Delta^2 u_h b_{\mathbf{x}_0} \, d\mathbf{x} - \sum_{e \in \mathcal{F}_I} \left(\int_e \llbracket \nabla(\Delta u_h) \rrbracket b_{\mathbf{x}_0} \, ds - \int_e \llbracket \Delta u_h \rrbracket \cdot \nabla b_{\mathbf{x}_0} \, ds \right) \\
&\leq \|\Delta^2 u_h\|_{L^2(\omega_{K_0})} \|b_{\mathbf{x}_0}\|_{L^2(\omega_{K_0})} + \sum_{e \in \mathcal{F}_I} \|\llbracket \nabla(\Delta u_h) \rrbracket\|_{L^2(e)} \|b_{\mathbf{x}_0}\|_{L^2(e)} + \sum_{e \in \mathcal{F}_I} \|\llbracket \Delta u_h \rrbracket\|_{L^2(e)} \|\nabla b_{\mathbf{x}_0}\|_{L^2(e)} \\
&\leq Ch_{K_0}^{-1} \left(h_{K_0}^2 \|\Delta^2 u_h\|_{L^2(\omega_{K_0})} + \sum_{e \in \mathcal{F}_I} h_e^{3/2} \|\llbracket \nabla(\Delta u_h) \rrbracket\|_{L^2(e)} + \sum_{e \in \mathcal{F}_I} h_e^{1/2} \|\llbracket \Delta u_h \rrbracket\|_{L^2(e)} \right). \tag{3.60}
\end{aligned}$$

Inserting (3.60) into (3.59) yields

$$\begin{aligned}
1 &\leq Ch_{K_0}^{-1} \left(|u - u_h|_{H^2(\omega_{K_0})} + h_K^2 \|\Delta^2 u_h\|_{L^2(\omega_{K_0})} \right. \\
&\quad \left. + \sum_{e \in \mathcal{F}_I} h_e^{3/2} \|\llbracket \nabla(\Delta u_h) \rrbracket\|_{L^2(e)} + \sum_{e \in \mathcal{F}_I} h_e^{1/2} \|\llbracket \Delta u_h \rrbracket\|_{L^2(e)} \right), \tag{3.61}
\end{aligned}$$

which, together with (3.48), (3.53), and (3.58), implies

$$h_{K_0} \leq C|||u - u_h|||_{\omega_{K_0}}. \tag{3.62}$$

The estimate (3.45) follows from (3.48), (3.53), (3.58), and (3.62).

If $\mathbf{x}_0 \in \mathcal{N}$, for $\forall K \in \mathcal{T}_h$, the term h_K vanishes in η_K and the estimation (3.45) reduces to

$$\left(\eta_{1,K}^2 + \sum_{e \in \mathcal{E}_K \cap \mathcal{E}_I} \alpha_e \eta_{3,e}^2 + \sum_{e \in \mathcal{E}_K \cap \mathcal{E}_I} \alpha_e \eta_{4,e}^2 \right)^{1/2} \leq C|||u - u_h|||_{\omega_K}. \tag{3.63}$$

Then, the estimate (3.63) is given directly by (3.48), (3.53) and (3.58). \square

3.2. A posteriori error estimation based on regularized problem. Inspired by the technique of second-order elliptic equations with a Dirac delta source term, as discussed in [23], where the L^2 projection of the Dirac delta function is used to produce a regular solution, allowing adaptive procedures based on standard a posteriori error estimators to work efficiently. This regularization approach using projection techniques can also be applied for the problem (1.1).

More specifically, the Dirac delta function can be approximated by $\delta_h \in V_{h,0}^m \subset H_0^1(\Omega)$, defined as

$$\delta_h = \begin{cases} 0, & \text{in } \Omega \setminus \overline{K_0}, \\ \delta_{K_0}, & \text{in } K_0, \end{cases}$$

where $\delta_{K_0} \in P_m(K_0)$ satisfying

$$\int_{K_0} \delta_{K_0} v \, d\mathbf{x} = v(\mathbf{x}_0), \quad \forall v \in P_m(K_0).$$

Therefore, it holds

$$\int_{\Omega} \delta_h v \, d\mathbf{x} = v(\mathbf{x}_0).$$

Let us consider the ensuing auxiliary problem:

$$\Delta^2 \bar{u} = \delta_h \quad \text{in } \Omega, \quad \bar{u} = 0 \quad \text{and} \quad \partial_{\mathbf{n}} \bar{u} = 0 \quad \text{on } \partial\Omega. \quad (3.64)$$

The C^0 interior penalty method for problem (3.64) is to find $\bar{u}_h \in V_{h,0}^m$ such that

$$A_h(\bar{u}_h, v_h) = v(\mathbf{x}_0) = \int_{\Omega} \delta_h v_h \, d\mathbf{x} \quad \forall v_h \in V_{h,0}^m. \quad (3.65)$$

The well-posedness of the scheme (3.65) follows from the Lax-Milgram theorem. Let u and \bar{u} be exact solutions for the original problem (1.1) and auxiliary problem (3.64), respectively. Let \bar{u}_h be corresponding numerical solutions of (3.65). The error estimate can be decomposed into two parts using the triangular inequality

$$|u - \bar{u}_h|_{H^2(\Omega)} \leq |u - \bar{u}|_{H^2(\Omega)} + |\bar{u} - \bar{u}_h|_{H^2(\Omega)}. \quad (3.66)$$

The first term represents the regularization error, while the second term represents the discretization error. We estimate the total error by summing the independent contributions from each part.

Based on the regularity of the solution to (3.64), the discretization error can be estimated as [33, 8]

$$|\bar{u} - \bar{u}_h|_{H^2(\Omega)} \leq Ch^{\min\{1, \alpha\}}. \quad (3.67)$$

where $\alpha < \alpha_0$ with α_0 given in (2.4).

The error estimate (3.66) will be dominated by the regularization error. Referring to [33], the following projection error bound holds

$$|\delta_{\mathbf{x}_0} - \delta_h|_{H^{-r}(\Omega)} \leq Ch^{r-1}, \quad 1 < r \leq m, \quad (3.68)$$

where m is the degree of the polynomial. Using the elliptic regularity theory and (3.68) yield

$$|u - \bar{u}|_{H^2(\Omega)} \leq C|\delta_{\mathbf{x}_0} - \delta_h|_{H^{-2}(\Omega)} \leq Ch_{K_0}. \quad (3.69)$$

Based on (3.66), (3.67), and (3.69), we have the following result.

Lemma 3.11. Let \mathcal{T}_h be the quasi-uniform triangulation with mesh size h , and let u and \bar{u}_h be solutions of (1.1) and (3.65), respectively. Then the following error estimate holds

$$|u - \bar{u}_h|_{H^2(\Omega)} \leq Ch^{\min\{1, \alpha\}}.$$

Remark 3.12. Two techniques are employed in the C^0 interior penalty method to solve problem (1.1): a direct method (2.9) and a method using the projection technique (3.65). By comparing the error estimates of the solutions obtained with the direct method (see Lemma 2.7) and with the projection technique (see Lemma 3.11), we observe that solutions from both techniques exhibit the same convergence rate on quasi-uniform meshes.

Based on the projection technique, we propose the second residual-based a posteriori error estimator for the C^0 interior penalty method solving problem (1.1) as

$$\xi(\bar{u}_h) = \left(h_{K_0}^2 + \sum_{K \in \mathcal{T}_h} \xi_K^2(\bar{u}_h) \right)^{1/2}, \quad (3.70)$$

the local indicator ξ_K is given by

$$\xi_K(\bar{u}_h) = \begin{cases} \left(h_{K_0}^2 + \bar{\xi}_{K_0}^2 \right)^{1/2}, & \text{if } K = K_0, \\ \bar{\xi}_K, & \text{if } K \in \Omega \setminus K_0, \end{cases} \quad (3.71)$$

where

$$\xi_K(\bar{u}_h) = \left(\xi_{1,K}^2 + \sum_{e \in \mathcal{E}_K \cap \mathcal{E}_h} \alpha_e \xi_{2,e}^2 + \sum_{e \in \mathcal{E}_K \cap \mathcal{E}_I} \alpha_e \xi_{3,e}^2 + \sum_{e \in \mathcal{E}_K \cap \mathcal{E}_I} \alpha_e \xi_{4,e}^2 \right)^{1/2}, \quad (3.72)$$

with $\alpha_e = 1$ for $e \in \mathcal{E}_B$, $\alpha_e = 1/2$ for $e \in \mathcal{E}_I$, and

$$\begin{aligned} \xi_{1,K} &= h_K^2 \|\delta_h - \Delta^2 \bar{u}_h\|_{L^2(K)}, & \xi_{2,e} &= \beta h_e^{-1/2} \|[\![\nabla \bar{u}_h]\!] \|_{L^2(e)}, \\ \xi_{3,e} &= h_e^{1/2} \|[\![\Delta \bar{u}_h]\!] \|_{L^2(e)}, & \xi_{4,e} &= h_e^{3/2} \|[\![\nabla \Delta \bar{u}_h]\!] \|_{L^2(e)}. \end{aligned}$$

The corresponding global upper and local lower bounds are given as follows.

Theorem 3.13 (Reliability). Let u and \bar{u} be exact solutions for the original problem (1.1) and auxiliary problem (3.64), respectively. And $\bar{u}_h \in V_{h,0}^m$ is the solution of (3.65). Then the residual-based a posteriori error estimator ξ satisfies the global bound

$$|||u - \bar{u}_h||| \leq C\xi. \quad (3.73)$$

Proof. By triangular inequality, the left hand side of (3.73) is bounded from above by

$$|||u - \bar{u}_h||| \leq |||u - \bar{u}||| + |||\bar{u} - \bar{u}_h|||.$$

Using the elliptic regularity bound, Lemma 3.3 and (3.69), the first term can be estimated as follows

$$|||u - \bar{u}|||^2 = \sum_{K \in \mathcal{T}_h} |u - \bar{u}|_{H^2(K)}^2 + \sum_{e \in \mathcal{E}_h} \frac{\beta}{h_e} \|[\![\nabla(u - \bar{u})]\!] \|_{L^2(e)}^2 = |u - \bar{u}|_{H^2(\Omega)}^2 \leq Ch_{K_0}^2. \quad (3.74)$$

Similar to the proof of Theorem 3.4, to prove $|||\bar{u} - \bar{u}_h||| \leq C\xi$, it is sufficient to verify that

$$\left(\sum_{K \in \mathcal{T}_h} |\bar{u} - \chi|_{H^2(K)}^2 \right)^{1/2} \leq \sup_{\phi \in H_0^2(\Omega) \setminus \{0\}} \frac{a(\bar{u} - \chi, \phi)}{|\phi|_{H^2(\Omega)}} \leq C\xi, \quad (3.75)$$

where $\chi = E_h \bar{u}_h \in H_0^2(\Omega)$. Let $\phi_I \in V_{h,0}^m$ be the continuous interpolation polynomial of ϕ . Then,

$$a(\bar{u} - \chi, \phi) = \sum_{K \in \mathcal{T}_h} \int_K (\delta_h - \Delta^2 \bar{u}_h)(\phi - \phi_I) \, dx + L_h, \quad (3.76)$$

where

$$\begin{aligned} L_h &= a_h(\bar{u}_h - \chi, \phi) + \sum_{e \in \mathcal{E}_I} \int_e [[\nabla(\Delta \bar{u}_h)]] (\phi - \phi_I) \, ds - \sum_{e \in \mathcal{E}_I} \int_e [[\Delta \bar{u}_h]] \cdot \{ \{ \nabla(\phi - \phi_I) \} \} \, ds \\ &\quad - \sum_{e \in \mathcal{E}_h} \int_e [[\nabla \bar{u}_h]] \{ \{ \Delta \phi_I \} \} \, ds + \sum_{e \in \mathcal{E}_h} \frac{\beta}{h_e} \int_e [[\nabla \bar{u}_h]] [[\nabla \phi_I]] \, ds \end{aligned}$$

satisfies

$$L_h \leq C \left(\sum_{e \in \mathcal{E}_h} \xi_{2,e}^2 + \sum_{e \in \mathcal{E}_I} \xi_{3,e}^2 + \sum_{e \in \mathcal{E}_I} \xi_{4,e}^2 \right)^{1/2} |\phi|_{H^2(\Omega)}. \quad (3.77)$$

By the Cauchy-Schwarz inequality and Lemma 2.6, the first term in (3.76) follows

$$\begin{aligned} \sum_{K \in \mathcal{T}_h} \int_K (\delta_h - \Delta^2 \bar{u}_h) (\phi - \phi_I) \, d\mathbf{x} &\leq \sum_{K \in \mathcal{T}_h} \|\delta_h - \Delta^2 \bar{u}_h\|_{L^2(K)} \|\phi - \phi_I\|_{L^2(K)} \\ &\leq C \sum_{K \in \mathcal{T}_h} h_K^2 \|\delta_h - \Delta^2 \bar{u}_h\|_{L^2(K)} |\phi|_{H^2(K)} \leq C \left(\sum_{K \in \mathcal{T}_h} \xi_{1,K}^2 \right)^{1/2} |\phi|_{H^2(\Omega)}, \end{aligned} \quad (3.78)$$

which together with (3.74) and (3.77) yields the conclusion. \square

Theorem 3.14 (Efficiency). For the local indicator ξ_K defined in (3.71), there exists a positive constant C independent of the mesh size such that

$$\xi_K \leq \begin{cases} C \left(h_{K_0} + \| |u - \bar{u}_h| \|_{\omega_{K_0}} \right), & K = K_0, \\ C \| |u - \bar{u}_h| \|_{\omega_K}, & K \in \mathcal{T}_h \setminus K_0. \end{cases} \quad (3.79)$$

Proof. Let's first show the element residual term $\xi_{1,K} = h_K^2 \|\delta_h - \Delta^2 \bar{u}_h\|_{L^2(K)}$ satisfies the estimate (3.79). For $\forall v \in V_{h,0}^m$, using integration by part gives

$$\begin{aligned} \int_K (\delta_h - \Delta^2 \bar{u}_h) v \, d\mathbf{x} &= \int_K (\delta_h - \delta_{\mathbf{x}_0}) v \, d\mathbf{x} + \int_K \Delta^2 (u - \bar{u}_h) v \, d\mathbf{x} \\ &= \int_K (\delta_h - \delta_{\mathbf{x}_0}) v \, d\mathbf{x} + \int_K \Delta (u - \bar{u}_h) \Delta v \, d\mathbf{x} \\ &\quad - \int_{\partial K} \Delta (u - \bar{u}_h) \mathbf{n} \cdot \nabla v \, ds + \int_{\partial K} \nabla \Delta (u - \bar{u}_h) \cdot \mathbf{n} v \, ds. \end{aligned} \quad (3.80)$$

We set $v|_K = (\delta_h - \Delta^2 \bar{u}_h) b_K^2$ in (3.80), where $v \in H_0^2(\Omega) \cap H_0^2(K)$ and satisfies $v = 0$ in $\Omega \setminus K$. Noticing that $v|_e = \nabla v|_e = 0$. Consequently, (3.80) yields

$$\int_K (\delta_h - \Delta^2 \bar{u}_h) v \, d\mathbf{x} = \int_K (\delta_h - \delta_{\mathbf{x}_0}) v \, d\mathbf{x} + \int_K \Delta (u - \bar{u}_h) \Delta v \, d\mathbf{x}.$$

By Lemma 3.5, it holds

$$\|v\|_{L^2(K)} \leq C \|\delta_h - \Delta^2 \bar{u}_h\|_{L^2(K)}.$$

We prove the first case in (3.79), i.e., $K = K_0$. By Cauchy-Schwarz inequality, Lemma 2.5 and (3.69),

$$\begin{aligned} \int_{K_0} (\delta_h - \Delta^2 \bar{u}_h) v \, d\mathbf{x} &\leq (\|\delta_h - \delta_{\mathbf{x}_0}\|_{H^{-2}(K_0)} + \|\Delta (u - \bar{u}_h)\|_{L^2(K_0)}) \|v\|_{H^2(K_0)} \\ &\leq C h_{K_0}^{-2} \left(h_{K_0} + \| |u - \bar{u}_h| \|_{H^2(\omega_{K_0})} \right) \|v\|_{L^2(K_0)}. \end{aligned} \quad (3.81)$$

By (3.31) and (3.81), it holds

$$\begin{aligned} \|\delta_h - \Delta^2 \bar{u}_h\|_{L^2(K_0)}^2 &\leq C \int_{K_0} (\delta_h - \Delta^2 \bar{u}_h)^2 b_{K_0}^2 \, d\mathbf{x} = C \int_{K_0} (\delta_h - \Delta^2 \bar{u}_h) v \, d\mathbf{x} \\ &\leq Ch_{K_0}^{-2} \left(h_{K_0} + |u - \bar{u}_h|_{H^2(\omega_{K_0})} \right) \|\delta_h - \Delta^2 \bar{u}_h\|_{L^2(K_0)}, \end{aligned}$$

which implies

$$h_{K_0}^2 \|\delta_h - \Delta^2 \bar{u}_h\|_{L^2(K_0)} \leq C \left(h_{K_0} + |u - \bar{u}_h|_{H^2(\omega_{K_0})} \right). \quad (3.82)$$

Note that $(\delta_h - \delta_{\mathbf{x}_0})|_K = 0$ for any $K \in \mathcal{T}_h \setminus K_0$. Similar to the proof of the first case in (3.79), it follows

$$h_K^2 \|\delta_h - \Delta^2 \bar{u}_h\|_{L^2(K)} \leq C |u - \bar{u}_h|_{H^2(\omega_K)}. \quad (3.83)$$

Verifying other terms in ξ_K can refer to the proof of Theorem 3.10. \square

3.3. Adaptive finite element algorithm. The adaptive finite element algorithm based on the residual-based a posteriori error estimator (3.5) or (3.70) is summarized as follows.

Algorithm 1 The adaptive finite element algorithm.

- 1: Input: an initial mesh \mathcal{T}_h^0 ; a constant $0 < \theta \leq 1$; the maximum number of mesh refinements n .
 - 2: Output: the numerical solution u_h^n (resp. \bar{u}_h^n); a new refined mesh \mathcal{T}_h^n .
 - 3: for $i = 0$ to n do
 - Solve the discrete equation for the finite element solution u_h^i (resp. \bar{u}_h^i) on \mathcal{T}_h^i ;
 - Computing the local and total error estimation $\eta_K^i(u_h^i)$ (resp. $\xi_K^i(\bar{u}_h^i)$) and $\eta^i(u_h^i)$ (resp. $\xi^i(\bar{u}_h^i)$);
 - if $i < n$ then
 - Select a subset $\widetilde{\mathcal{T}}_h^i \subset \mathcal{T}_h^i$ of marked elements to refined such that,

$$\left(\sum_{K \in \widetilde{\mathcal{T}}_h^i} \eta_K^i(u_h^i)^2 \right)^{1/2} \geq \theta \eta^i(u_h^i), \quad \left(\text{resp.} \quad \left(\sum_{K \in \widetilde{\mathcal{T}}_h^i} \xi_K^i(\bar{u}_h^i)^2 \right)^{1/2} \geq \theta \xi^i(\bar{u}_h^i) \right);$$
 - Refine the each element $K \in \widetilde{\mathcal{T}}_h^i$ by longest edge bisection to obtain a new mesh \mathcal{T}_h^{i+1} .
 - end if
 - end for
-

4. EXTENSIONS

In this section, we extend our results to cover a broader class of fourth-order elliptic equations with various boundary conditions. Specifically, we generalize the biharmonic operator Δ^2 in (1.1) to a more general fourth order operator \mathcal{L} that includes low order terms

$$\mathcal{L}u = \Delta^2 u - \mu_1 \Delta u + \mu_2 u, \quad (4.1)$$

where $\mu_\ell \geq 0$ (for $\ell = 1, 2$) are constants. Both residual-based a posteriori error estimators, (3.1) and (3.71), for problem (1.1) can be extended to the new operator. We only present the first type residual-based a posteriori error estimator for simplicity. The proofs of the efficiency and reliability are expected to be similar to those provided in Section 3. Therefore, we will focus solely on presenting the corresponding a posteriori error estimators and leave their performance to be verified numerically.

4.1. Non-homogeneous Dirichlet boundary conditions. Consider the following problem:

$$\Delta^2 u - \mu_1 \Delta u + \mu_2 u = \delta_{\mathbf{x}_0} + f \quad \text{in } \Omega, \quad u = g \quad \text{and} \quad \partial_{\mathbf{n}} u = g_N \quad \text{on } \partial\Omega, \quad (4.2)$$

where g_D and g_N are given functions on the boundary $\partial\Omega$, and f is a given function in the domain Ω . We assume that g , g_N , and f are sufficiently smooth. This problem is a scalar analog of the variational problem for the strain gradient theory in elasticity and plasticity [35] when the coefficients satisfy $\mu_1 > 0$ and $\mu_2 = 0$.

In [8], a C^0 interior penalty method was proposed to solve the general fourth-order elliptic equation without the Dirac delta function term $\delta_{\mathbf{x}_0}$. In the subsequent section, we extend and adapt this method to handle the presence of the Dirac delta function term $\delta_{\mathbf{x}_0}$ on the right-hand side of equation (4.2).

We define the space V_h^m associated with the triangulation \mathcal{T}_h by

$$V_h^m = \{v_h \in H^1(\Omega) \cap C^0(\Omega) : v_h|_K \in P_m(K), m \geq 2, \quad \forall K \in \mathcal{T}_h\}. \quad (4.3)$$

Denote the subspace of V_h^m by

$$V_{h,g}^m = \{v_h \in V_h^m : v_h|_{\partial\Omega} = \mathcal{I}_h g\}, \quad (4.4)$$

where $\mathcal{I}_h g \in V_h^m$ is a polynomial approximation function of g by the interpolation on the boundary.

The C^0 interior penalty method for (4.2) is to find $u_h \in V_{h,g}^m$ such that

$$\begin{aligned} & \sum_{K \in \mathcal{T}_h} \left(\int_K \Delta u_h \Delta v_h \, d\mathbf{x} + \mu_1 \int_K \nabla u_h \cdot \nabla v_h \, d\mathbf{x} + \mu_2 \int_K u_h v_h \, d\mathbf{x} \right) + \sum_{e \in \mathcal{E}_h} \frac{\beta}{h_e} \int_e [[\nabla u_h]] [[\nabla v_h]] \, ds \\ & - \sum_{e \in \mathcal{E}_h} \left(\int_e \{ \{ \Delta u_h \} \} [[\nabla v_h]] \, ds + \int_e \{ \{ \Delta v_h \} \} [[\nabla u_h]] \, ds \right) \\ & = v(\mathbf{x}_0) + \sum_{K \in \mathcal{T}_h} \int_K f v \, d\mathbf{x} - \sum_{e \in \mathcal{E}_B} \int_e g_N \Delta v \, ds + \sum_{e \in \mathcal{E}_B} \frac{\beta}{h_e} \int_e g_N \nabla v \cdot \mathbf{n} \, ds, \quad \forall v_h \in V_{h,0}^m, \end{aligned} \quad (4.5)$$

where $V_{h,0}^m$ is defined as (2.6).

Unlike the C^0 interior penalty method for problems with homogeneous Dirichlet boundary conditions described in (2.9), the modified method (4.5) incorporates additional boundary term. These additional terms account for the non-homogeneous nature of the boundary conditions. The local error estimator on $K \in \mathcal{T}_h$ for C^0 interior penalty method (4.2) is given by

$$\eta_K(u_h) = \begin{cases} (h_{K_0}^2 + \tilde{\eta}_{K_0}^2)^{1/2}, & \text{if } K = K_0 \text{ and } \mathbf{x}_0 \notin \mathcal{N}, \\ \tilde{\eta}_K, & \text{otherwise,} \end{cases} \quad (4.6)$$

where

$$\begin{aligned} \tilde{\eta}_K(u_h) = & \left(\tilde{\eta}_{1,K}^2 + \sum_{e \in \mathcal{E}_K \cap \mathcal{E}_I} \gamma_e \eta_{2,e}^2 + \sum_{e \in \mathcal{E}_K \cap \mathcal{E}_I} \alpha_e \eta_{3,e}^2 + \sum_{e \in \mathcal{E}_K \cap \mathcal{E}_I} \alpha_e \eta_{4,e}^2 \right. \\ & \left. + \sum_{e \in \mathcal{E}_K \cap \mathcal{E}_B} \gamma_e \eta_{5,e}^2 + \sum_{e \in \mathcal{E}_K \cap \mathcal{E}_B} \gamma_e \eta_{6,e}^2 \right)^{1/2}, \end{aligned} \quad (4.7)$$

with $\gamma_e = (1 + \mu_1 h_e^2 + \mu_2 h_e^4) \alpha_e$, $\alpha_e = 1$ for $e \in \mathcal{E}_B$, $\alpha_e = 1/2$ for $e \in \mathcal{E}_I$, and

$$\tilde{\eta}_{1,K}^2 = h_K^4 \|f - \Delta^2 u_h + \mu_1 \Delta u_h - \mu_2 u_h\|_{L^2(K)}^2, \quad (4.8)$$

$$\eta_{5,e}^2 = \beta h_e^{-1/2} \|g_N - \nabla u_h \cdot \mathbf{n}\|_{L^2(e)}^2, \quad (4.9)$$

$$\eta_{6,e}^2 = h_e^{-3/2} \|g - u_h\|_{L^2(e)}^2. \quad (4.10)$$

and $\eta_{2,e}, \eta_{3,e}$ and $\eta_{4,e}$ are given in (3.3)-(3.4).

4.2. Navier boundary conditions. We also extend the results to the fourth order equation with Navier boundary conditions,

$$\Delta^2 u - \mu_1 \Delta u + \mu_2 u = \delta_{\mathbf{x}_0} + f \quad \text{in } \Omega, \quad u = g \quad \text{and} \quad \Delta u = g_B \quad \text{on } \partial\Omega, \quad (4.11)$$

where g and g_B are given functions on the boundary $\partial\Omega$, and f is a given function within the domain Ω . We also assume that g , g_B , and f are sufficiently smooth. The problem (4.11) models a simply supported plate problem [34]. When the Dirac delta function term $\delta_{\mathbf{x}_0}$ vanishes, [10] studied a symmetric C^0 interior penalty method for a fourth-order singular perturbation elliptic problem with these types of boundary conditions in two dimensions on polygonal domains. The C^0 interior penalty method for (4.11) is to find $u_h \in V_{h,g}^m$ such that

$$\begin{aligned} & \sum_{K \in \mathcal{T}_h} \left(\int_K \Delta u_h \Delta v_h \, d\mathbf{x} + \mu_1 \int_K \nabla u_h \cdot \nabla v_h \, d\mathbf{x} + \mu_2 \int_K u_h v_h \, d\mathbf{x} \right) + \sum_{e \in \mathcal{E}_I} \frac{\beta}{h_e} \int_e \llbracket \nabla u_h \rrbracket \llbracket \nabla v_h \rrbracket \, ds \\ & - \sum_{e \in \mathcal{E}_I} \left(\int_e \{\{ \Delta u_h \} \} \llbracket \nabla v_h \rrbracket \, ds + \int_e \{\{ \Delta v_h \} \} \llbracket \nabla u_h \rrbracket \, ds \right) \\ & = v(\mathbf{x}_0) + \sum_{K \in \mathcal{T}_h} \int_K f v \, d\mathbf{x} + \sum_{e \in \mathcal{E}_B} \int_e g_B \nabla v \cdot \mathbf{n} \, ds. \quad \forall v_h \in V_{h,0}^m, \end{aligned} \quad (4.12)$$

where V_h^m is defined as (2.6). The local error estimator for the C^0 interior penalty method (4.12) is given by

$$\eta_K(u_h) = \begin{cases} (h_{K_0}^2 + \zeta_{K_0}^2)^{1/2}, & \text{if } K = K_0 \text{ and } \mathbf{x}_0 \notin \mathcal{N}, \\ \zeta_K, & \text{otherwise,} \end{cases} \quad (4.13)$$

where

$$\begin{aligned} \zeta_K(u_h) = & \left(\tilde{\eta}_{1,K}^2 + \sum_{e \in \mathcal{E}_K \cap \mathcal{E}_h} \gamma_e \eta_{2,e}^2 + \sum_{e \in \mathcal{E}_K \cap \mathcal{E}_I} \alpha_e \eta_{3,e}^2 + \sum_{e \in \mathcal{E}_K \cap \mathcal{E}_I} \alpha_e \eta_{4,e}^2 \right. \\ & \left. + \sum_{e \in \mathcal{E}_K \cap \mathcal{E}_B} \zeta_{5,e}^2 + \sum_{e \in \mathcal{E}_K \cap \mathcal{E}_B} \gamma_e \eta_{6,e}^2 \right)^{1/2}, \end{aligned} \quad (4.14)$$

the element residual $\tilde{\eta}_{1,K}$ and the edge residuals $\eta_{2,e}, \eta_{3,e}, \eta_{4,e}, \eta_{6,e}$ are defined as (4.7). The boundary residual term $\zeta_{5,e}$ is defined by

$$\zeta_{5,e}^2 = h_e^{1/2} \|g_B - \Delta u_h\|_{L^2(e)}^2. \quad (4.15)$$

4.3. Homogeneous Neumann boundary conditions. For fourth-order elliptic equations with homogeneous Neumann boundary conditions, we consider the following model

$$\Delta^2 u - \mu_1 \Delta u + \mu_2 u = \delta_{\mathbf{x}_1} - \delta_{\mathbf{x}_0} \quad \text{in } \Omega, \quad \partial_{\mathbf{n}} u = 0 \quad \text{and} \quad \partial_{\mathbf{n}}(\Delta u) = 0 \quad \text{on } \partial\Omega. \quad (4.16)$$

where $\mathbf{x}_0, \mathbf{x}_1$ represent two distinct points strictly contained in the domain Ω . These boundary-value problems can arise in the Cahn-Hilliard model, which describes phase-separation phenomena [14]. [9] proposed a quadratic C^0 interior penalty method for fourth-order boundary value problems with similar types of boundary conditions, assuming the right-hand side function $f \in L^2(\Omega)$. Under these conditions, a unique solution u can be found, satisfying $u \in H^{2+\alpha}(\Omega)$ for $\alpha \in (0, 2]$.

It is straightforward to validate the solvability condition:

$$\int_{\Omega} \delta_{\mathbf{x}_1} - \delta_{\mathbf{x}_0} \, dx = 0.$$

To obtain a unique solution, a common approach is to impose an additional constraint

$$\int_{\Omega} u \, dx = 0.$$

We define a subspace of $H^1(\Omega)$ by

$$V = \{v_h \in H^1(\Omega) : \partial_{\mathbf{n}} v_h = 0, \int_{\Omega} v_h \, dx = 0\}.$$

The finite element space X_h^m associated with the triangulation \mathcal{T}_h is defined as

$$X_h^m = \{v_h \in V \cap C^0(\Omega) : v_h|_K \in P_m(K), m \geq 2, \quad \forall K \in \mathcal{T}_h\}. \quad (4.17)$$

The C^0 interior penalty method for (4.16) is then to find $u_h \in X_h^m$ such that

$$\begin{aligned} & \sum_{K \in \mathcal{T}_h} \left(\int_K \Delta u_h \Delta v_h \, d\mathbf{x} + \mu_1 \int_K \nabla u_h \cdot \nabla v_h \, d\mathbf{x} + \mu_2 \int_K u_h v_h \, d\mathbf{x} \right) + \sum_{e \in \mathcal{E}_h} \frac{\beta}{h_e} \int_e \llbracket \nabla u_h \rrbracket \llbracket \nabla v_h \rrbracket \, ds \\ & - \sum_{e \in \mathcal{E}_h} \left(\int_e \{\{\Delta u_h\}\} \llbracket \nabla v_h \rrbracket \, ds + \int_e \{\{\Delta v_h\}\} \llbracket \nabla u_h \rrbracket \, ds \right) = v(\mathbf{x}_1) - v(\mathbf{x}_0). \quad \forall v_h \in X_h^m, \end{aligned} \quad (4.18)$$

Note that the bilinear in (4.18) is identical to that in (4.5), with the exception that the finite element space now includes only functions with a zero mean value.

Denote $K_1 \in \mathcal{T}_h$ by one element such that the singular point $\mathbf{x}_1 \in \overline{K_1}$, where $\overline{K_1}$ is the closure of K_1 . The diameter of K_1 is denoted by h_{K_1} . The local error estimator for problem (4.11) is given by

$$\eta_K(u_h) = \begin{cases} (h_{K_0}^2 + \chi_{K_0}^2)^{1/2}, & \text{if } K = K_0, \text{ and } \mathbf{x}_0 \notin \mathcal{N}, \\ (h_{K_1}^2 + \chi_{K_1}^2)^{1/2}, & \text{if } K = K_1, \text{ and } \mathbf{x}_1 \notin \mathcal{N}, \\ \chi_K, & \text{otherwise.} \end{cases} \quad (4.19)$$

where

$$\chi_K(u_h) = \left(\tilde{\eta}_{1,K}^2 + \sum_{e \in \mathcal{E}_K \cap \mathcal{E}_h} \gamma_e \eta_{2,e}^2 + \sum_{e \in \mathcal{E}_K \cap \mathcal{E}_I} \alpha_e \eta_{3,e}^2 + \sum_{e \in \mathcal{E}_K \cap \mathcal{E}_I} \alpha_e \eta_{4,e}^2 \right). \quad (4.20)$$

The definition of $\chi_K(u_h)$ is same as $\zeta_K(u_h)$ in (4.14), except for discarding the the boundary residual term $\zeta_{5,e}$.

5. NUMERICAL EXAMPLES

In this section, we present numerical test results to verify the accuracy of the C^0 interior penalty method and demonstrate the robustness of the proposed residual-type a posteriori estimators. If the exact solution u is given, the convergence rate is calculated by

$$\mathcal{R} = \log_2 \frac{|u - u_h^{j-1}|_{H^2(\Omega)}}{|u - u_h^j|_{H^2(\Omega)}}, \quad (5.1)$$

where u_h^j is the C^0 finite element solution on the mesh \mathcal{T}_h^j obtained after j th refinements of the initial triangulation \mathcal{T}_h^0 . When the exact solution is unavailable or difficult to obtain, we instead use the following numerical convergence rate

$$\mathcal{R} = \log_2 \frac{|u_h^j - u_h^{j-1}|_{H^2(\Omega)}}{|u_h^{j+1} - u_h^j|_{H^2(\Omega)}}. \quad (5.2)$$

Due to the lack of regularity, the C^0 interior penalty method with high-degree polynomial approximations on quasi-uniform triangular meshes may not achieve optimal convergence rates. To address this, we apply an adaptive C^0 interior penalty method to improve the convergence order.

The convergence rate of the a posteriori error estimator η (resp. ξ) for P_m polynomials with $m \geq 2$ is quasi-optimal if

$$\eta \approx N^{-0.5(m-1)} \quad (\text{resp. } \xi \approx N^{-0.5(m-1)}).$$

Here and in what follows, we abuse the notation N to represent the total number of degrees of freedom.

Example 5.1 (L-shape domain). We consider problem (1.1) with homogeneous clamped boundary conditions in an L-shaped domain $\Omega = (-2\pi, 2\pi)^2 \setminus [0, 2\pi) \times (-2\pi, 0]$ with a largest interior angle $\omega = 3\pi/2$. The Dirac point $\mathbf{x}_0 = (-\pi, \pi)$, then the solution show singularities at two points $(0, 0)$ and \mathbf{x}_0 . We start with an initial mesh \mathcal{T}_h^0 as Figure 4(a).

TABLE 2. Example 5.1: Convergence rate of numerical solution in uniform meshes.

	P_2				P_3				P_4			
j	4	5	6	7	3	4	5	6	3	4	5	6
\mathcal{R}	0.88	0.85	0.80	0.73	1.00	0.73	0.60	0.56	0.74	0.58	0.56	0.55

Table 2 shows the H^2 convergence history using the P_m -based C^0 interior penalty method on quasi-uniform meshes, with $m = 2, 3, 4$. From the results, we observe that the convergence rates are $\mathcal{R} < 1$ on coarse meshes, and $\mathcal{R} \approx 0.5445$ on sufficiently refined meshes. This indicates that the singularity in the solution is primarily influenced by the reentrant corner of the polygonal domain when $\omega > \pi$. The results in Table 2 align with the theoretical expectations outlined in Lemma 2.2.

We then assess the efficiency of the a posteriori error estimators. Meshes generated by η in (3.5) and ξ in (3.70) are shown Figure 5 and Figure 6, respectively. It is evident that the error estimators effectively guide mesh refinements around the points $(0, 0)$ and $(-\pi, \pi)$, where the solution shows singularities. As shown in Figure 7, the slopes for the estimators are close to $-0.5(m - 1)$ when there are sufficient grid points, indicating optimal decay of the error with respect to the number of unknowns. The contours of the corresponding numerical solutions based on η and ξ are shown in Figure 4(b)-(c), they are very similar.

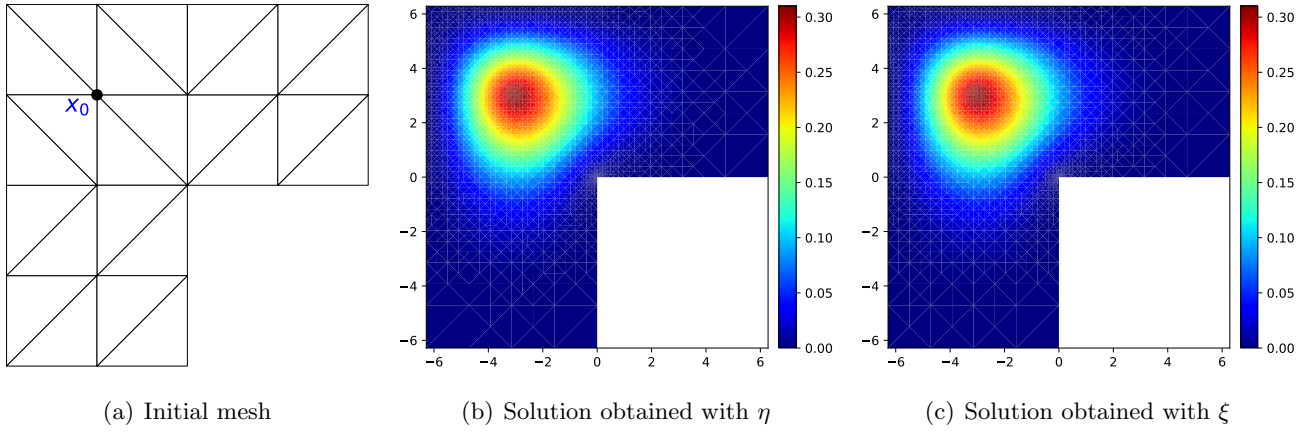
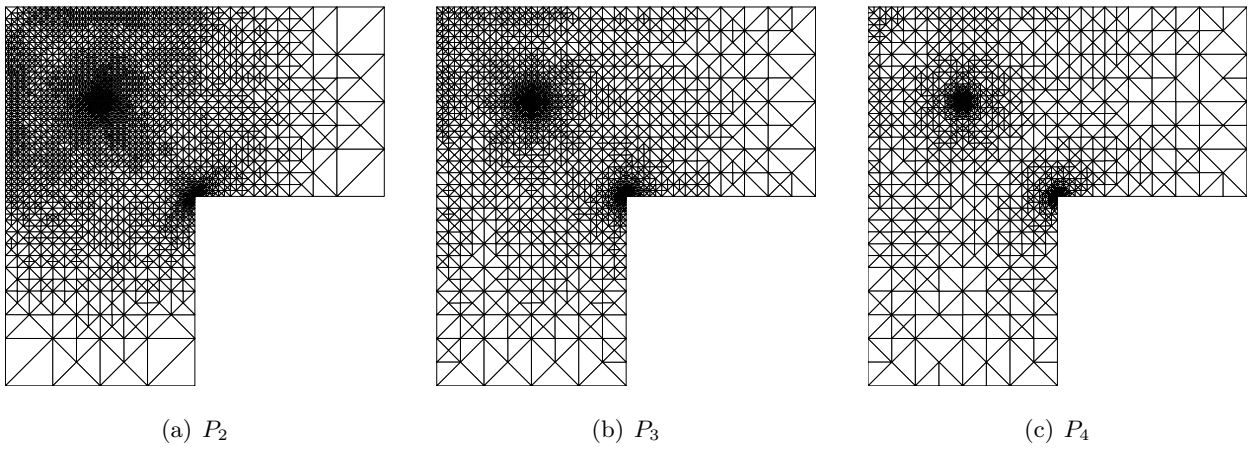
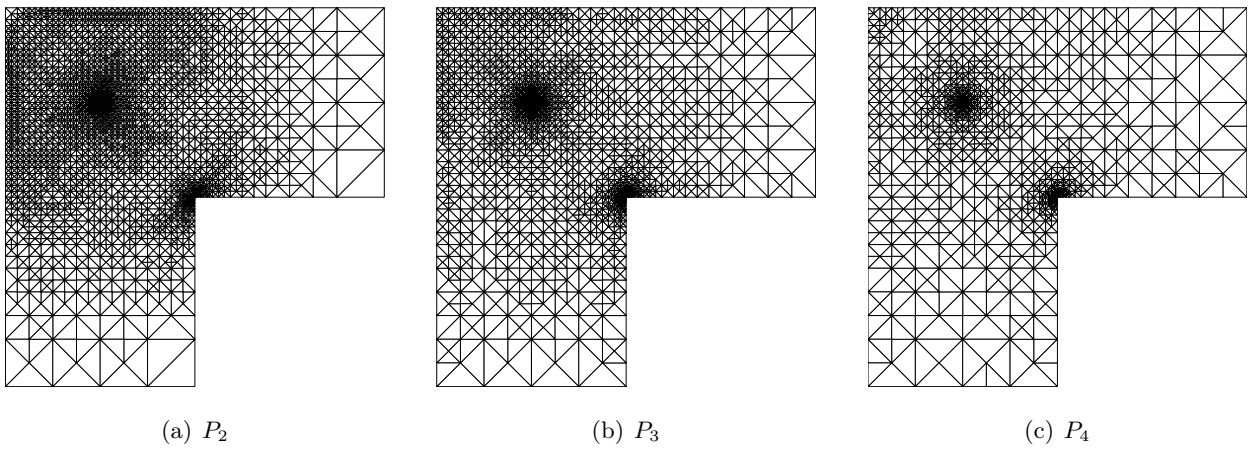


FIGURE 4. Example 5.1: initial mesh and adaptive numerical solution.

FIGURE 5. Example 5.1: adaptive meshes generated by η .FIGURE 6. Example 5.1: adaptive meshes generated by ξ .

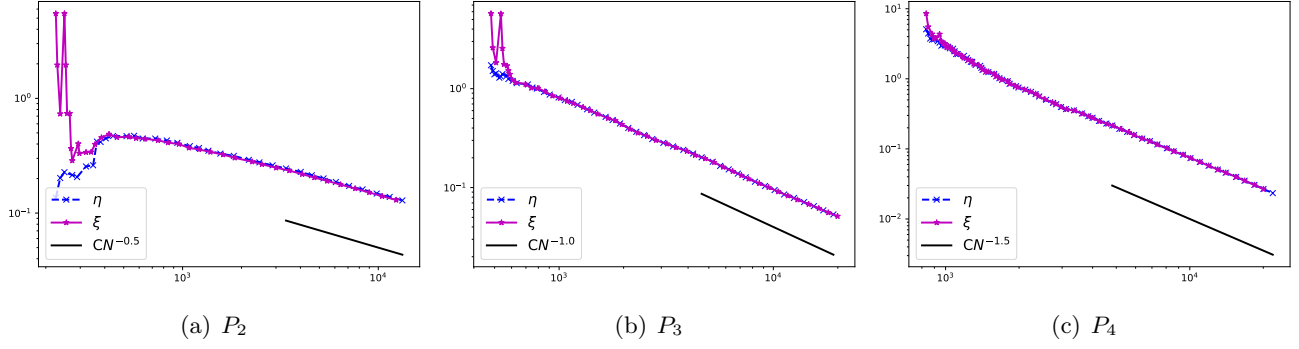


FIGURE 7. Example 5.1: error estimators.

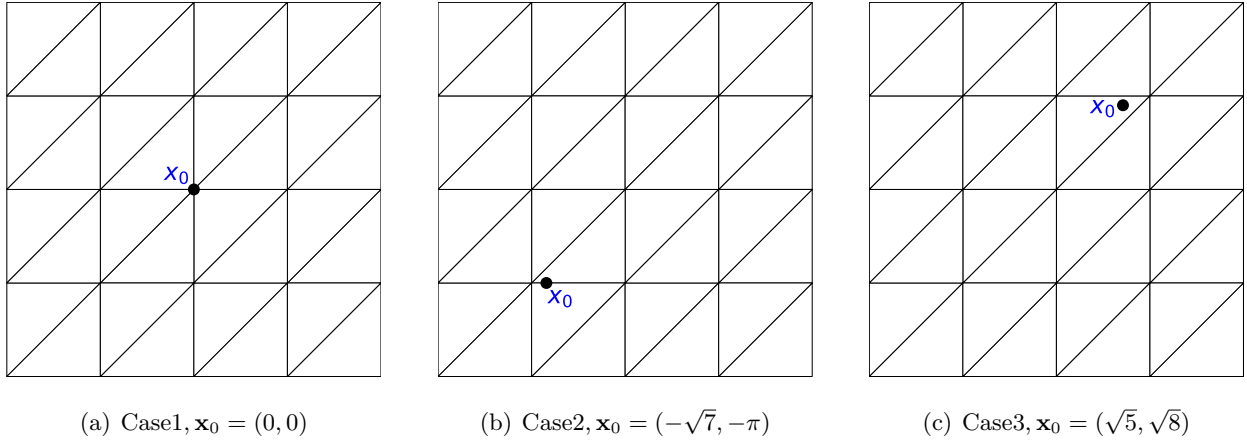


FIGURE 8. Example 5.2: initial meshes.

Example 5.2 (Non-homogeneous boundary). In this example, we consider a more general biharmonic equation

$$\Delta^2 u - \mu_1 \Delta u + \mu_2 u = \delta_{\mathbf{x}_0} + f, \quad (5.3)$$

where the location of \mathbf{x}_0 in \mathcal{T}_h are of three different types as shown in Case 1-3. The initial meshes of Cases 1-3 are reported in Figure 8.

Case 1: $\mathbf{x}_0 = (0, 0)$ is a node of the triangulations.

Case 2: $\mathbf{x}_0 = (-\sqrt{7}, -\pi)$ belongs to an inter edge $e \in \mathcal{E}_I$.

Case 3: $\mathbf{x}_0 = (\sqrt{5}, \sqrt{8})$ is contained by one element $K \in \mathcal{T}_h$.

We take the function

$$f(x, y) = \mu_2 \frac{|\mathbf{x} - \mathbf{x}_0|^2}{8\pi} \ln |\mathbf{x} - \mathbf{x}_0| - \mu_1 \left(\frac{\ln |\mathbf{x} - \mathbf{x}_0|}{2\pi} + \frac{1}{2\pi} \right), \quad (5.4)$$

then the exact solution of equation (5.3) is given by

$$u(x, y) = \frac{|\mathbf{x} - \mathbf{x}_0|^2}{8\pi} \ln |\mathbf{x} - \mathbf{x}_0|. \quad (5.5)$$

We consider (5.3) with two different boundary conditions and the parameters in $u(x, y)$ are taken as $\mu_1 = \mu_2 = 1$.

TABLE 3. Example 5.2 Test 1: Convergence rate of numerical solution in uniform meshes.

	P_2				P_3				P_4			
j	4	5	6	7	3	4	5	6	2	3	4	5
Case 1	0.99	0.99	1.00	1.00	1.60	1.41	1.18	1.06	1.97	1.59	1.14	1.02
Case 2	0.98	0.99	0.99	1.00	1.67	1.72	1.20	0.96	1.72	1.59	1.35	0.87
Case 3	0.98	0.99	0.99	1.00	1.68	1.72	1.33	1.23	1.93	1.60	1.32	0.94

TABLE 4. Example 5.2 Test 2: Convergence rate of numerical solution in uniform meshes.

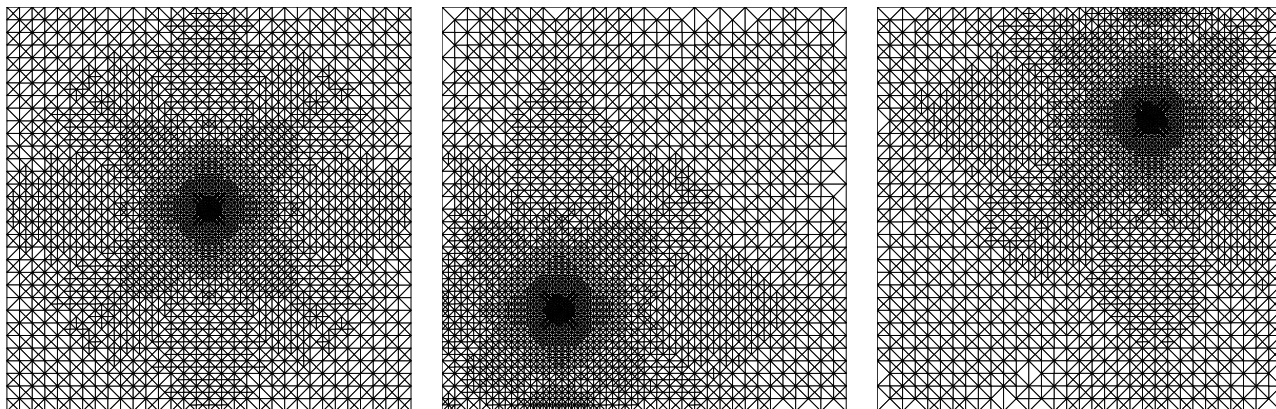
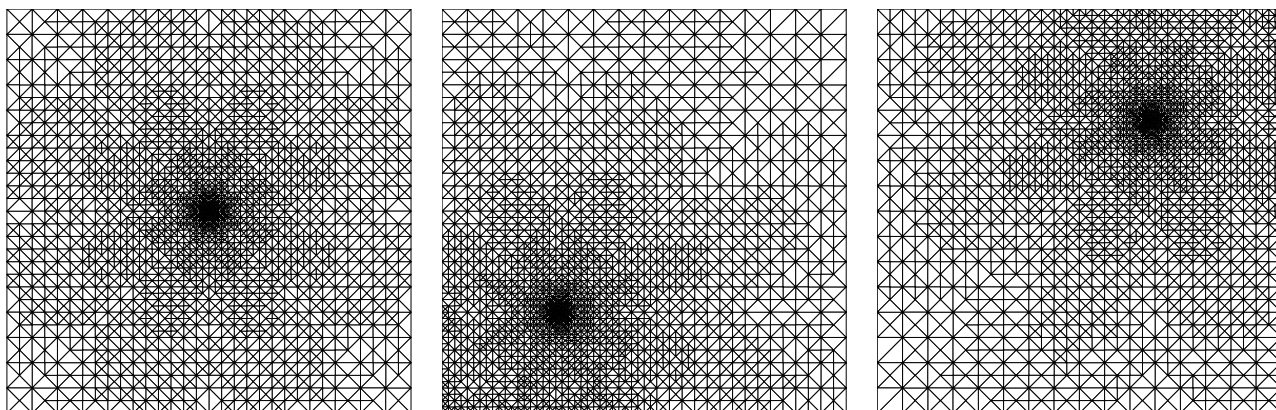
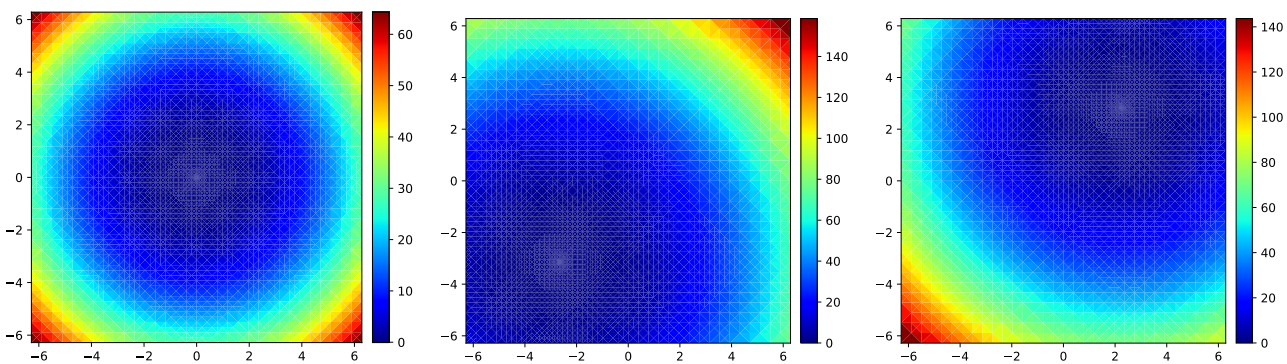
	P_2				P_3				P_4			
j	4	5	6	7	3	4	5	6	2	3	4	5
Case 1	0.99	0.99	1.00	1.00	1.60	1.41	1.18	1.06	1.97	1.59	1.14	1.02
Case 2	0.98	1.00	0.99	1.00	1.67	1.72	1.19	0.95	1.68	1.57	1.35	0.87
Case 3	0.99	0.99	0.99	1.00	1.71	1.75	1.33	1.23	1.94	1.58	1.32	0.94

Test 1. We first consider non-homogeneous campled boundary conditions. The convergence rates of the C^0 interior penalty method solutions based on P_2 , P_3 and P_4 polynomials for Case 1-3 in quasi-uniform meshes are shown in Table 3. The convergence rates are approximately $\mathcal{R} \approx 1$. While the convergence rates for P_2 are quasi-optimal, the rates for P_3 , P_4 only achieve suboptimal convergence. This is due to $u \in H^{3-\epsilon}(\Omega)$ for $\omega = \frac{\pi}{2}$. Given the low regularity of the solution u , these results are the best that can be achieved with quasi-uniform meshes.

To address this, we apply the adaptive C^0 interior penalty method based on the residual-based a posteriori error estimator η_K in (4.6). The corresponding numerical solutions of the adaptive algorithm using the error estimator η are presented in Figure 11. Figure 9 and Figure 10 show the adaptive meshes of P_3 , P_4 approximations, respectively. The error estimator effectively guides mesh refinements, particularly around the point \mathbf{x}_0 . The convergence rates of the error estimator η based on P_3 , P_4 polynomials are illustrated in Figures 12(a)-(b), respectively. These results suggest that the convergence rates of η are quasi-optimal for all three cases. Furthermore, with mesh refinement, the convergence slopes of the error estimators for Cases 1-3 nearly coincide. This demonstrates the superior performance of the adaptive algorithm based on the a posteriori error indicator presented in this work, especially when compared with uniform refinement.

Test 2. We set the non-homogeneous Navier boundary conditions. Similar to Test 1, we apply both the C^0 interior penalty method and the adaptive C^0 interior penalty method to this problem. Numerical results on uniform meshes are listed in Table 4. We perform P_3 and P_4 polynomial approximations using the adaptive C^0 interior penalty method, with the numerical results displayed in Figures 13-16. The results obtained are similar to those in Test 1. As mentioned earlier, (i) the convergence rates on uniform meshes are $\mathcal{R} \approx 1$; (ii) the position of the Dirac point within the cell has a negligible effect on the convergence rates, whether the meshes are adaptively refined or uniformly refined; (iii) refinements are concentrated around the point \mathbf{x}_0 ; (iv) The convergence rates of η are quasi-optimal.

Example 5.3 (Homogeneous Neumann boundary). For the final example, we consider problem (4.16) with homogeneous Neumann boundary on convex domain $\Omega = (-2\pi, 2\pi) \times (-2\pi, 2\pi)$. The right-hand side function is given as $\delta_{\mathbf{x}_1} - \delta_{\mathbf{x}_0}$, where $\mathbf{x}_0 = (-\pi, 0)$, $\mathbf{x}_1 = (\pi, 0)$. An initial uniform triangular mesh \mathcal{T}_h^0 is shown in Figure 17(a).

(a) Case 1, $x_0 = (0, 0)$ (b) Case 2, $x_0 = (-\sqrt{7}, -\pi)$ (c) Case 3, $x_0 = (\sqrt{5}, \sqrt{8})$ FIGURE 9. Example 5.2 Test 1: adaptive meshes for P_3 .(a) Case 1, $x_0 = (0, 0)$ (b) Case 2, $x_0 = (-\sqrt{7}, -\pi)$ (c) Case 3, $x_0 = (\sqrt{5}, \sqrt{8})$ FIGURE 10. Example 5.2 Test 1: adaptive meshes for P_4 .(a) Case 1, $x_0 = (0, 0)$ (b) Case 2, $x_0 = (-\sqrt{7}, -\pi)$ (c) Case 3, $x_0 = (\sqrt{5}, \sqrt{8})$ FIGURE 11. Example 5.2 Test 1: adaptive solution for P_3 .

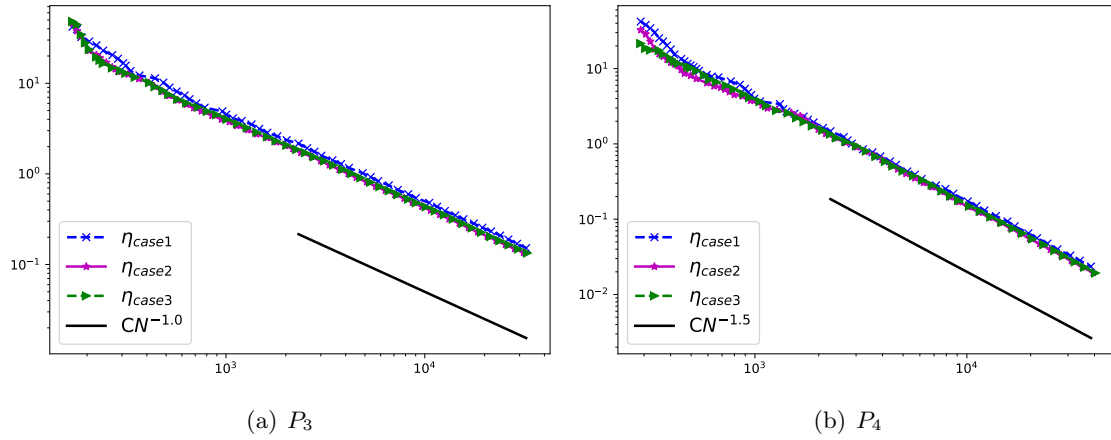
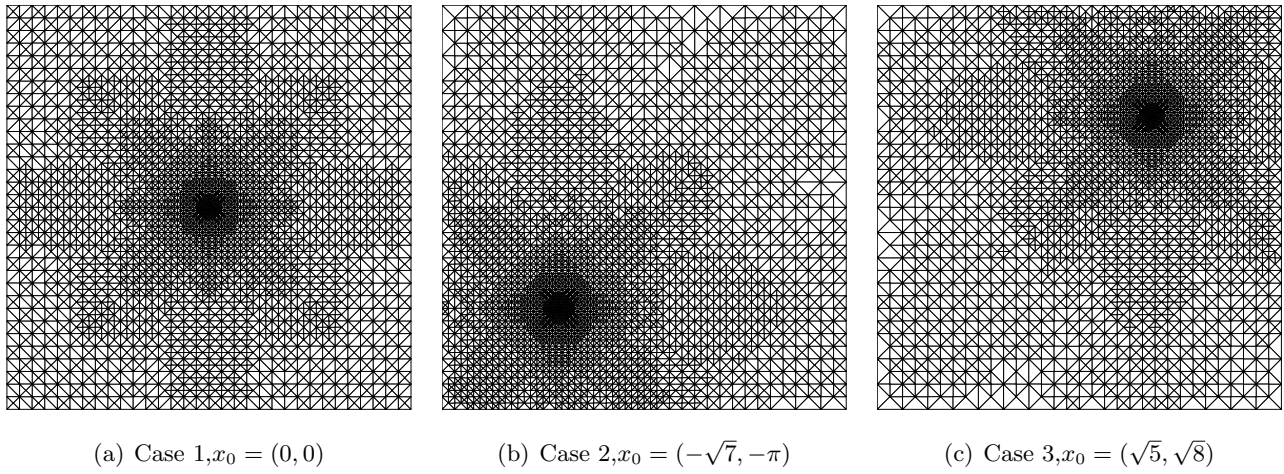
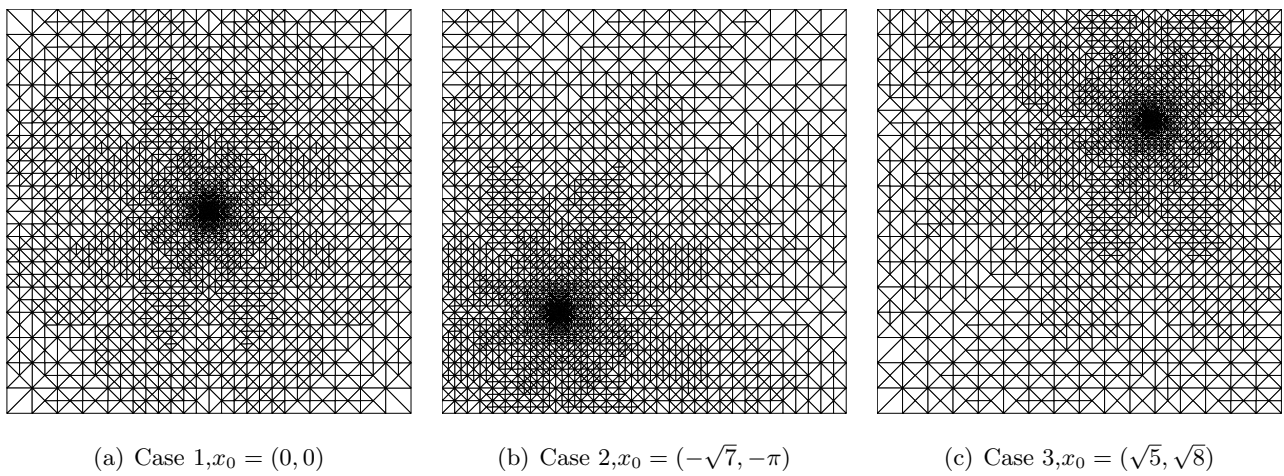


FIGURE 12. Example 5.2 Test 1: error estimators.

FIGURE 13. Example 5.2 Test 2: adaptive meshes for P_3 .FIGURE 14. Example 5.2 Test 2: adaptive meshes for P_4 .

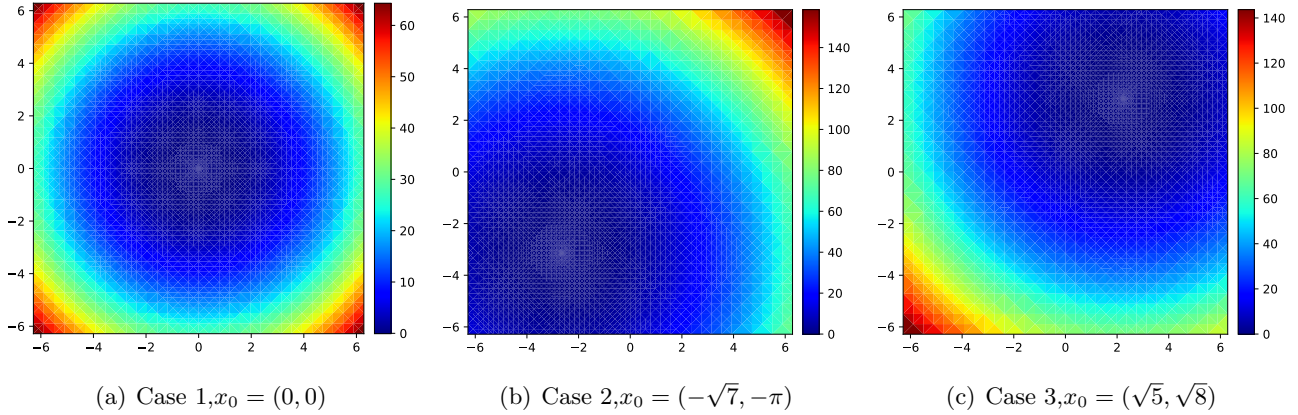
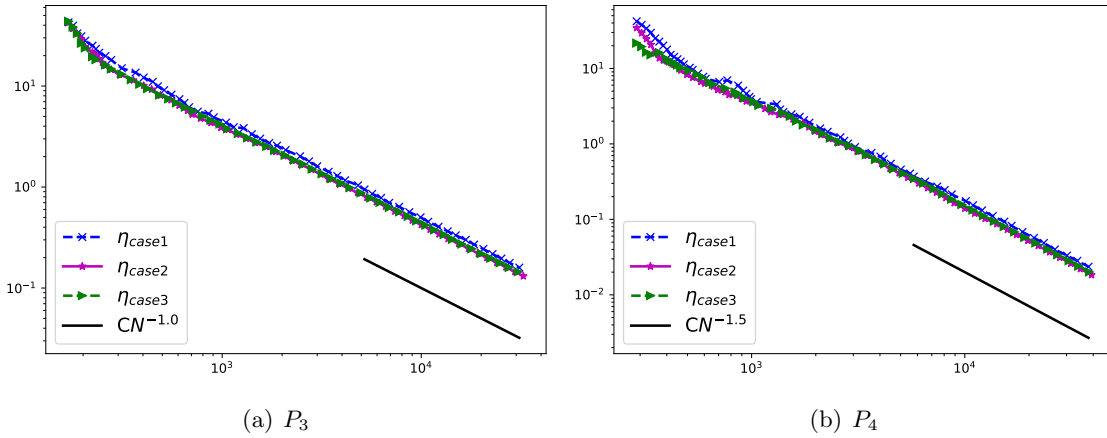
FIGURE 15. Example 5.2 Test 2: adaptive solution for P_3 .

FIGURE 16. Example 5.2 Test 2: error estimators.

TABLE 5. Example 5.3: Convergence rate of numerical solution in uniform meshes.

	P_2				P_3				P_4			
j	4	5	6	7	3	4	5	6	2	3	4	5
\mathcal{R}	0.87	0.90	0.91	0.92	1.00	1.00	1.00	1.00	1.00	1.00	1.00	1.00

The convergence rates of the C^0 interior penalty method solutions based on P_m , $m = 2, 3, 4$ polynomials on quasi-uniform meshes are shown in Table 5. We observe that $\mathcal{R} \approx 1$. Due to the low global regularity of the solution, the convergence rates on quasi-uniform meshes can not reach the optimal order for P_3 , P_4 polynomial approximations. For enhanced accuracy, the adaptive C^0 interior penalty method is better suited for this type of problem. The contour of adaptive C^0 interior penalty method approximation based on P_3 is shown in Figure 17(a). Figure 17(b)-(c) show the adaptive meshes of P_3 , P_4 polynomial approximations, respectively. We can see clearly that the error estimator guides the mesh refinement densely around the points \mathbf{x}_0 and \mathbf{x}_1 . The convergence rates of error estimator η based on P_3 , P_4 polynomials are shown Figure 18(b)-(c). These results align with expectations, indicating that the convergence rates of the error estimator are quasi-optimal.

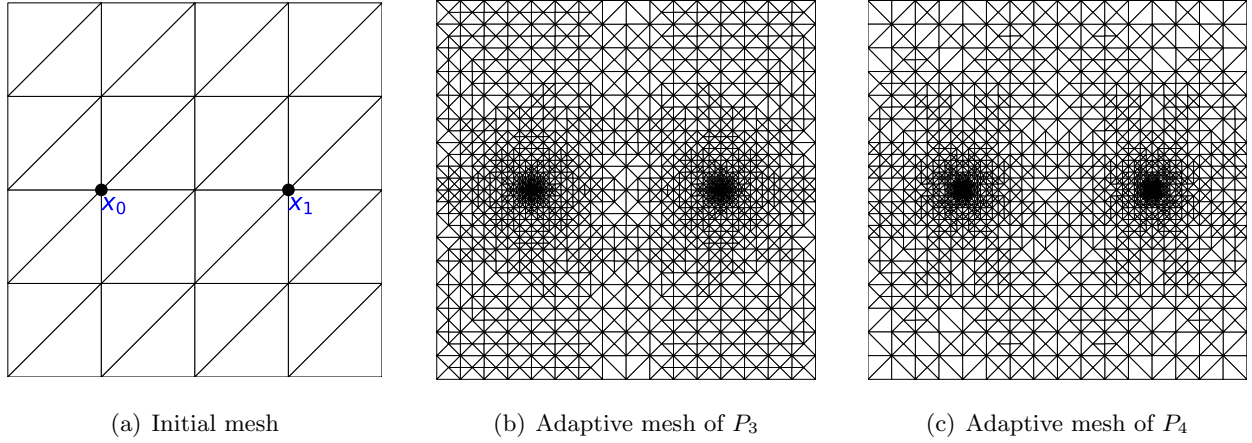


FIGURE 17. Example 5.3: initial mesh and adaptive meshes.

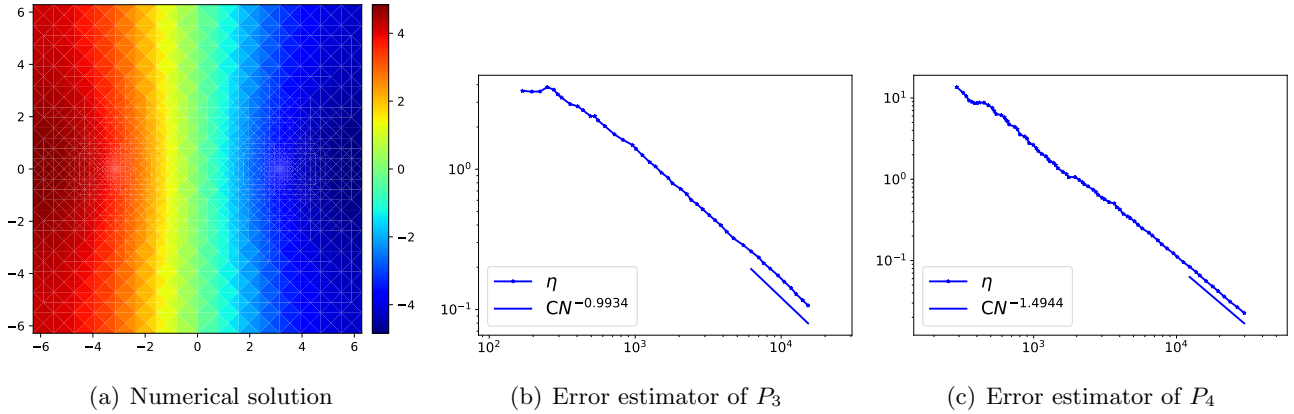


FIGURE 18. Example 5.1: numerical solution and error estimators.

6. CONCLUSION

Two residual-based a posteriori estimators are proposed for biharmonic problem (1.1). The first estimator is directly derived from the model equation, while the second estimator is based on the projection of the Dirac delta function onto the discrete finite element space. The later one introduces an additional projection error, which is included in the error estimator, yielding a similar effect to the first estimator in guiding mesh refinement. For both a posteriori estimators, we rigorously prove that these estimators are efficient and reliable. An adaptive C^0 interior penalty algorithm is provided based on the proposed a posteriori estimators. Extensions of the first estimator to more general fourth order elliptic equations are provided, and quasi-optimal convergence rates are numerically observed.

ACKNOWLEDGMENTS

Y. Huang was supported in part by NSFC Project (12431014), Project of Scientific Research Fund of Hunan Provincial Science and Technology Department (2020ZYT003). N. Yi was supported by NSFC Project (12071400), Project of Scientific Research Fund of the Hunan Provincial Science and Technology Department (2024ZL5017), and Program for Science and Technology Innovative Research Team in Higher Educational Institutions of Hunan Province of China.

DATA AVAILABILITY

Enquiries about data availability should be directed to the authors.

DECLARATIONS

The authors declare that they have no conflict of interest.

REFERENCES

- [1] R. Araya, E. Behrens, and R. Rodríguez. A posteriori error estimates for elliptic problems with Dirac delta source terms. *Numerische Mathematik*, 105(2):193-216, 2006.
- [2] R. Araya, E. Behrens, and R. Rodríguez. An adaptive stabilized finite element scheme for a water quality model. *Computer Methods in Applied Mechanics and Engineering*, 196(29-30):2800-2812, 2007.
- [3] J.H. Argyris, I. Fried and D.W. Scharpf. The TUBA family of plate elements for the matrix displacement method. *The Aeronautical Journal*, 72(692):701-709, 1968.
- [4] J.P. Agnelli, E.M. Garau and P. Morin A posteriori error estimates for elliptic problems with Dirac measure terms in weighted spaces. *ESAIM: Mathematical Modelling and Numerical Analysis*, 48(6):1557-1581,2014.
- [5] C. Bacuta and J.H. Bramble and J.E. Pasciak. Shift theorems for the biharmonic Dirichlet problem. *Springer*: 1-26,2002.
- [6] M. Bourlard and M. Dauge and M.S. Lubuma and S. Nicaise. Coefficients of the singularities for elliptic boundary value problems on domains with conical points. III: Finite element methods on polygonal domains. *SIAM Journal on Numerical Analysis*, 29(1):136-155, 1992.
- [7] S.C. Brenner, T. Gudi, and L.Y. Sung. An a posteriori error estimator for a quadratic C^0 -interior penalty method for the biharmonic problem. *IMA Journal of Numerical Analysis*, 30: 777–798, 2010.
- [8] S.C. Brenner and L.Y. Sung. C^0 interior penalty methods for fourth order elliptic boundary value problems on polygonal domains. *Journal of Scientific Computing*, 23(23): 83-118, 2005.
- [9] S.C. Brenner, S. Gu, T. Gudi and L.Y. Sung. A quadratic C^0 interior penalty method for linear fourth order boundary value problems with boundary conditions of the Cahn–Hilliard type. *SIAM Journal on Numerical Analysis*, 50(4): 2088-2110, 2012.
- [10] S.C. Brenner and M. Neilan. A C^0 interior penalty method for a fourth order elliptic singular perturbation problem. *SIAM Journal on Numerical Analysis*, 49(2): 869-892, 2011.
- [11] S. Brenner and L. Scott. The mathematical theory of finite element methods. *Volume 15 of Texts in Applied Mathematics*, 3rd edn. Springer, New York, 2008.
- [12] C. V. Camp. A solution of the nonhomogeneous biharmonic equation by the boundary element method. *Ph.D. thesis, Oklahoma State University*, 1987.
- [13] Philippe G. Ciarlet. The Finite Element Method for Elliptic Problems. *Université Pierre et Marie Curie, Paris, France*, 1974.
- [14] J. W. Cahn and J. E. Hilliard. Free energy of a nonuniform system-I: Interfacial free energy. *The Journal of Chemical Physics*, 28(2): 258-267, 1958.
- [15] J.T. Chen, H. Z. Liao and W.M. Lee An analytical approach for the Green’s functions of biharmonic problems with circular and annular domains. *Journal of Mechanics*, 25(1): 59-74,2011.
- [16] J.J. Douglas, T. Dupont, P. Percell and R. Scott. A family of C^1 finite elements with optimal approximation properties for various Galerkin methods for 2nd and 4th order problems. *RAIRO Analyse numérique*, 13(3):227–255, 1979.
- [17] G. Engel, K. Garikipati, T.J.R. Hughes, M.G. Larson, L. Mazzei and R.L. Taylor. Continuous/discontinuous finite element approximations of fourth-order elliptic problems in structural and continuum mechanics with applications to thin beams and plates, and strain gradient elasticity. *Computer methods in applied mechanics and engineering*, 191:3669-3750, 2002.
- [18] P. Grisvard. *Singularities in Boundary Value Problems*, volume 22 of *Research Notes in Applied Mathematics*. Springer-Verlag, New York, 1992.
- [19] W. Gong, M. Hinze and Z.J. Zhou. A priori error analysis for the finite element approximations of parabolic optimal control problems with pointwise control. *SIAM Journal on Control and Optimization*, 52(1):97-119, 2014.
- [20] E.H. Georgoulis, P. Houston and J. Virtanen. An a posteriori error indicator for discontinuous Galerkin approximations of fourth-order elliptic problems. *IMA Journal of Numerical Analysis*, 31:281-298, 2011.

- [21] F.D. Gaspoz, P.Morin and A, Veese. A posteriori error estimates with point sources in fractional sobolev spaces . *Numerical Methods for Partial Differential Equations*, 33(4):1018-1042,2016.
- [22] E.H. Georgoulis, P. Houston and J. Virtanen. An a posteriori error indicator for discontinuous Galerkin approximations of fourth-order elliptic problems. *IMA Journal of Numerical Analysis*, 31(1): 281–298, 2009.
- [23] P. Houston and T. Wihler. Discontinuous Galerkin methods for problems with Dirac delta source. *ESAIM: Mathematical Modelling and Numerical Analysis*, 46(6):1467-1483, 2012.
- [24] J. D. Jackson. Classical electrodynamics. *John Wiley and Sons, Inc., New York-London-Sydney*, second edition, 1975.
- [25] V.A. Kozlov, V.G. Maz'ya and J. Rossmann. Spectral problems associated with corner singularities of solutions to elliptic equations. *American Mathematical Society*, 85,2001.
- [26] S. B. G. Karakoc and M. Neilan. A C^0 finite element method for the Biharmonic problem without extrinsic penalization. *Numerical Methods for Partial Differential Equations*, 30(4),1254-1278,2014.
- [27] D. Leykekhman. Pointwise error estimates for C^0 interior penalty approximation of biharmonic problems. *Mathematics of Computation*, 90(327):41-63, 2020.
- [28] D. Leykekhman and B. Vexler. Optimal a priori error estimates of parabolic optimal control problems with pointwise control. *SIAM Journal on Numerical Analysis*, 51(5): 2797-2821, 2013.
- [29] H. Li, C. D. Wickramasinghe and P. Yin. A C^0 finite element method for the biharmonic problem with Dirichlet boundary conditions in a polygonal domain. *arXiv preprint arXiv:2207.03838*, 2022.
- [30] W. McLean. *Strongly Elliptic Systems and Boundary Integral Equations*. Cambridge University Press, 2000.
- [31] F. Millar, I.Muga, S Rojas and K.G. Van der Zee. Projection in negative norms and the regularization of rough linear functionals. *Numerische Mathematik*, 150: 1087-1121, 2022.
- [32] R. An and X.H. Huang. Constrained C^0 finite element methods for biharmonic problem. *Abstract and Applied Analysis*, 2012(137), 2012.
- [33] R. Scott. Finite element convergence for singular data. *Numerische Mathematik*, 21:317–327, 1973.
- [34] B. Semper. Conforming finite element approximations for a fourth-order singular perturbation problem. *SIAM Journal on Numerical Analysis*, 29(4): 1043-1058, 1992.
- [35] J.Y. Shu, W.E. King and N.A. Fleck. Finite elements for materials with strain gradient effects. *International Journal for Numerical Methods in Engineering*, 44(3): 373-391, 1999.
- [36] S. Timoshenko, S. Woinowsky-krieger. Theory of plates and shells. *McGraw-hill New York*, 1959.
- [37] F. Tan and Y. L. Zhang. The regular hybrid boundary node method in the bending analysis of thin plate structures subjected to a concentrated load. *European Journal of Mechanics A/Solids*, 38:79-89, 2013.

† HUNAN KEY LABORATORY FOR COMPUTATION AND SIMULATION IN SCIENCE AND ENGINEERING, SCHOOL OF MATHEMATICS AND COMPUTATIONAL SCIENCE, XIANGTAN UNIVERSITY, XIANGTAN 411105, HUNAN, P.R.CHINA

Email address: caohh@sustech.edu.cn (H. Cao); huangyq@xtu.edu.cn (Y. Huang); yinianyu@xtu.edu.cn (N. Yi).

* DEPARTMENT OF MATHEMATICAL SCIENCES, UNIVERSITY OF TEXAS AT EL PASO, EL PASO, TEXAS 79968, USA.

Email address: pyin@utep.edu